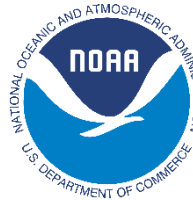# CDFW Contract E1696020

Linking predation mortality to predator density and survival for out-migrating Chinook Salmon and Steelhead in the lower San Joaquin River and South Delta

PI: Steven Lindley, NMFS-SWFSC Fisheries Ecology Division, steve.lindley@noaa.gov
Co PIs:
NMFS-SWFSC Fisheries Ecology Division/UC Santa Cruz
-Cyril Michel, cyril.michel@noaa.gov
-Nicholas Demetras, nicholas.demetras@noaa.gov
-Ilysa Iglesias, ilysa.iglesias@noaa.gov
-Brendan Lehman, brendan.lehman@noaa.gov

NMFS-NWFSC Point Adams Research Station
-David Huff, david.huff@noaa.gov
-Joseph Smith, joe.m.smith@noaa.gov

USGS Cooperative Fish and Wildlife Research Unit/Humboldt State University
-Mark Henderson, mark.henderson@humboldt.edu
-Christopher Loomis, christopher.loomis@humboldt.edu

Final Report

1. Introduction

Several native fish species that inhabit the rivers of California's Central Valley are in decline, and it is believed that one of the major contributors to these declines is low survival of these populations during residence in the Sacramento-San Joaquin River Delta. This is informed largely by tagging studies on juvenile salmonids that transit the Delta during their seaward migration (Kjelson and Brandes 1989, Perry 2010, Buchanan 2013). The exact mechanism of their mortality is unclear, but it is believed that a significant contributor is predation by the large populations of non-native piscine predators present in the Delta (Grossman et al. 2013). Significant interest exists in better understanding both the environmental drivers behind predation risk, as well as the relative importance of the contribution of predation to the mortality of these fish populations.

To date, while some studies have attempted to quantify the incidence of predators, prey, and piscivory items on a landscape scale in the Delta (Nobriga and Feyrer 2007), no empirical data exists on the environmental predictors of predator-prey dynamics at this scale; data which is critically needed to inform the numerous Delta-wide ecological models currently being developed and implemented for management purposes. We quantified predation risk, predator abundance, and relevant environmental covariates in the south Delta and lower San Joaquin River, and developed statistical relationships between them. Ultimately, our goal is to develop spatially and temporally-explicit predation risk estimates that will improve salmonid life-cycle modeling efforts currently underway in the Bay-Delta region. Additionally, predation risk estimates can also be compared to survival estimates of salmonid populations to discern what proportion of mortality is due to predation. Such information will allow for better predictions of the effectiveness and ecosystem-wide responses of management actions, including predator removals, habitat alteration, and water release strategies.

In this report, we outline predator abundances and density estimates as measured by Dual-Frequency Identification Sonar (DIDSON) cameras, spatial distribution of predation events as measured by Predation Event Recorders (PERs), and three different modeling exercises that used various habitat and water quality variables. We then used these models to predict: (1) predator densities, (2) seasonal changes in predation risk and (3) fine-scale (sub 1-km) spatial and temporal patterns in predation risk during the 2017 juvenile salmonid outmigration season. Finally, using the statistical relationships identified in the third model, we make preliminary efforts to predict predation risk at the 1-km resolution for the entire South Delta.

2. Methods

2.1. Field Site Selection

The Sacramento-San Joaquin Delta is a complex and expansive body of water, with over 1,100 km of waterways. While it would be ideal to investigate the predator-prey relationships throughout, such

an endeavor would be logistically challenging. Instead, we sampled sites in such a way as to extrapolate to the larger region in a statistically defensible manner. Specifically, we used Generalized Random Tesselation Stratified (GRTS) spatial sample selection (Stevens and Olson 2004). This method is a spatially-balanced sampling technique (i.e., approximately evenly dispersed over the extent of a region of interest) that allows for binning by sub-regions with similar characteristics (e.g., spatially grouped distributary waterways versus mainstem waterways). Therefore, site selection is still random and all regions of interest can be adequately sampled. This allows for defensible inferences over each individual region, and overall, the totality of the regions.

  Our study focused on the lower San Joaquin River and South Delta, a region of extremely low survival for outmigrating salmonids from the San Joaquin River drainage (Buchanan 2013). We delimited this area into 6 regions that share similar characteristics. The San Joaquin River was split into an Upper (from Mossdale to Stockton), Middle (from Stockton to Turner Cut) and Lower region (Turner Cut to Antioch). We delimited Old River into an Upper (Head of Old River to State Water Project) and a Lower region (State Water Project to confluence with the lower San Joaquin River). Finally, we sampled in one additional region that consisted of areas found between San Joaquin and Old Rivers that are geographically distinct from these two: Mildred Island, Turner Cut and Columbia Cut.

  The GRTS sample site selection method draws sites randomly and assigns them a draw number. We also drew extra sites beyond the number of sites we intended to visit ("oversampled sites") which we sampled only if any of the original sites were excluded due to logistical constraints. Once GRTS sample site selections were generated (Fig. 1), the first 21 draws were considered the tentative sites to be visited during the field season. We assessed these 21 sites for pairs of sites that were less than three river kilometers (kilometers by way of the river) away from each other. If we found such pairs, we dropped the site with the higher draw number and replaced it with a new site from the oversampled list. Of the 21 sites, three were selected that would be visited weekly in order to assess overall temporal trends in predation that should not be attributed to spatial trends ("repeat sites"). These three sites needed to be spatially-balanced in order to best capture temporal trends throughout the South Delta.
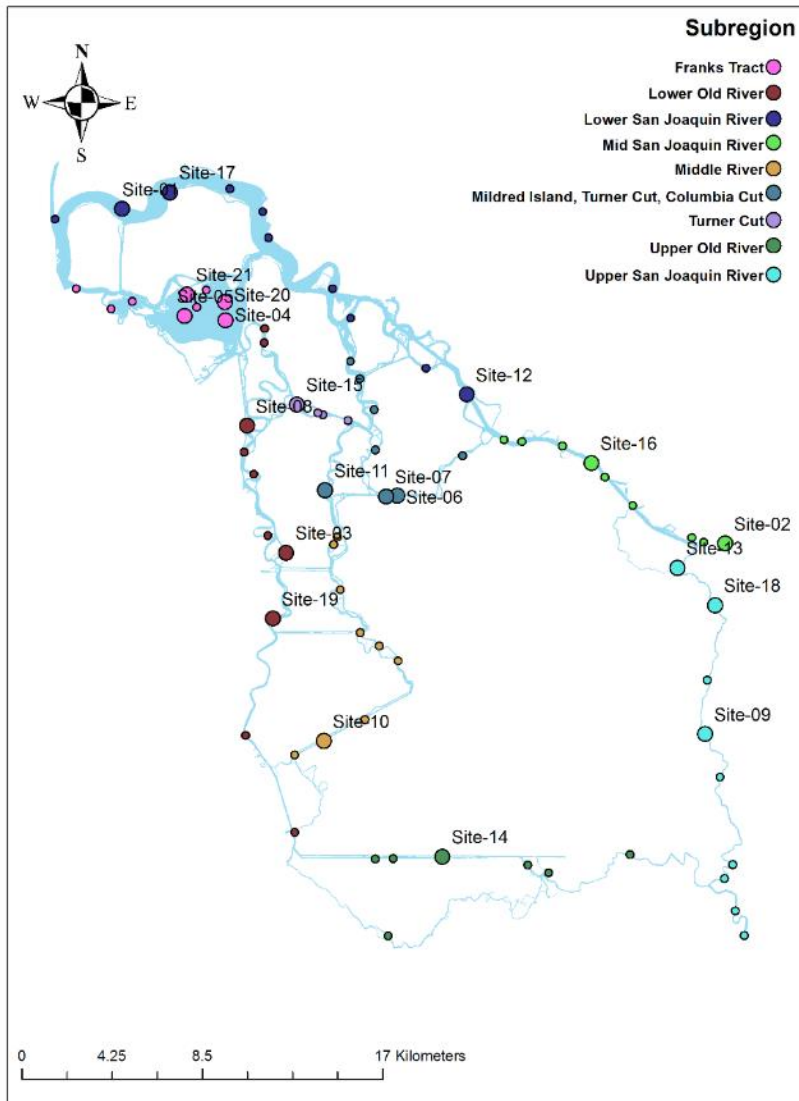
Figure 1. A map of the locations of the original site selection using GRTS method. Larger circles represent the first 21 main sites drawn and smaller circles represent surplus sites, which would have been visited in order of the draw number had a main site been deemed un-sampleable.

2.2. Predation Event Recorders

We developed Predation Event Recorders (PERs) to measure the relative predation rates on juvenile salmon swimming through our study reaches. PERs - described in detail in Demetras et al. (2016) - are drifting buoys with a live hatchery Chinook salmon *Oncorhynchus tshawytscha* smolt attached as bait. The drifting PERs were outfitted with a GPS tracker and predation-triggered timer that allowed us to determine the exact time and location of predation events (Fig. 2).
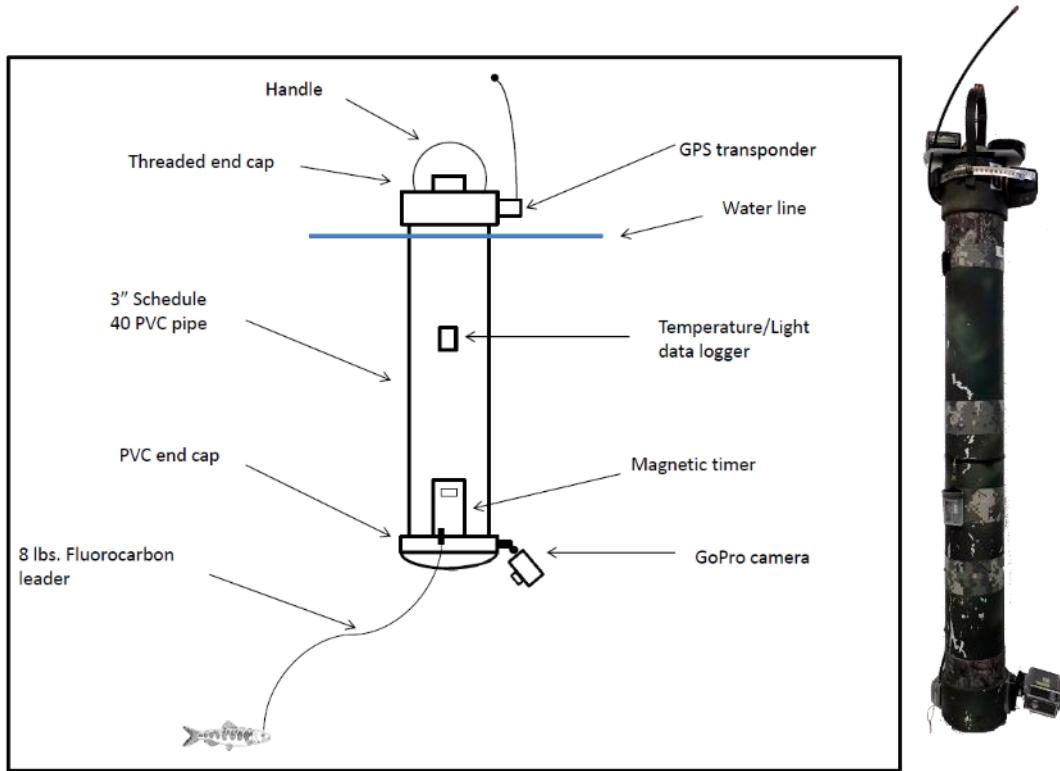
Figure 2. Schematic and picture of a floating PER.

Daily sampling occurred during a period that began approximately 3 hours before sunset and ended approximately 1.5 hours after. Previous studies have shown that predation risk is highest at sunset (Demetras et al. 2016); we wanted to amplify any potential predation risk to develop more robust relationships between predation risk and habitat and environmental variables. A boat-based crew would begin deploying floating PERs, 15 in total, at the upstream end of each 1-km study reach (as determined by the direction of current during that tide cycle). That boat would tend to the floating PERs as needed, dislodging them from submerged aquatic vegetation and re-deploying at the upstream end of the reach once they reached the end of the 1-km reach. Every time a PER was removed from the water, the status of the predation-triggered timer and Chinook salmon bait was recorded, the timer was reset, and the bait was replaced before redeployment if necessary.

PERs mounted and ready for deployment in the small boat "Heron" (E. Danner).

2.3. Estimating relative predation rates

We used a metric of percent predated PERs for graphical representations of the PER data. These were assessed through time (using the repeat sites by week) and through space (grouping sites by region). We considered each individual PER deployment as a repeated measure, and each of the sample sites as replicates. Therefore, we estimated the weekly or regional metric for percent predation per treatment type (wP) as the mean of the portion of PERs predated for each of the sample sites visited for the week or region, using formula below (eqn. 1):

$$(1) \qquad wP = \frac{\left[\sum_{i=1}^{N\ sample\ sites\ visited}\left(\frac{total\ predated\ PERs\ in\ site\ i}{total\ deployed\ PERs\ in\ site\ i}\right)\right]}{N\ sample\ sites\ visited} \times 100$$

Confidence intervals were estimated for each wP, using eqn. 2:

$$(2) \qquad 95\%\ confidence\ intervals\ for\ wP = wP \pm 1.96 \times Standard\ Error\ of\ the\ Mean$$

A measure of predation at any single sample site visit can be estimated using the percent of total deployed PERs that were predated on. However, error around this estimate alone cannot be calculated as it represents just one replicate, and therefore should only be used for assessing general trends in the data.

2.4. Habitat features and environmental variables

The distribution, behavior and abundance of both predator and prey fish species varies in response to environmental variables and the availability of suitable physical habitat features. In turn, predation rates likely vary in response to the heterogeneous nature of the surrounding physical environment. In order to examine relative predation rates upon juvenile Chinook salmon across the diverse spatial landscape of the Southern Delta, we measured environmental variables and quantified habitat metrics for each of our twenty study sites and incorporated these covariates into models of predator densities and predation risk. We selected environmental variables and habitat features known to exert influence over the relative abundance, energetic demands, and predator behavior and efficacy of predatory fresh water species present in the Southern Delta. Environmental variables were collected using both a water quality sonde (deployed in each study site for the duration of sampling) and temperature/light loggers that were attached to every PER. We quantified habitat features for each of our study sites using a combination of field collected and remote sensed data. For field sites, habitat data was collected and summarized to relevant spatial scales using Geographic Information System (GIS) mapping technology.

2.4.1. Submerged Aquatic Vegetation

Describing landscape-level habitat features with a low-cost side-scan fish finder sonar is a proven method for describing available habitat for fish within riverine systems (Kaeser et al. 2013 and Kaeser and Litts, 2010). We utilized side-scan sonar images to map the distribution of submerged aquatic vegetation (hereto referred to as SAV). The proliferation of non-native SAV in the Delta has been linked to the expansion of largemouth bass *Micropterus salmoides* populations (Conrad et al. 2016), and research indicates that SAV can locally modify habitat conditions within the Central Valley (Hestir et al. 2015). In addition, largemouth bass, a major predator within the Sacramento-San Joaquin system, tend to reside and forage within areas of dense vegetation (Savino and Stein 1989). In the Southern Sacramento-San Joaquin Delta, largemouth bass abundance is higher in areas dominated by SAV, while Chinook salmon and striped bass *Morone saxatilis*, are more likely to be found in turbid, open habitats (Nobriga et al. 2005). In order to account for the differential SAV habitat, we quantified the distribution and extent of SAV for each of our study sites in the field.

To measure SAV habitat per site, we ran parallel transects in the field, with a side-scan sonar transducer mounted on the hull of our vessel. Using an imaging display frequency of 455 kHz, we recorded images of the associated side-scan data, typically traversing the study site a minimum of three times (once per bank, and another pass through the middle of the channel, depending on the location). We then converted these images into GeoTiffs and hand digitized within ArcGIS (ESRI version 10.4.1) via visual estimation and ArcGIS editor tools. Prior to digitizing areas of SAV, we viewed side-scan images in real time in the field in order to develop a search image of these features. Only features (patches) greater than 5 meters along the longest axis were digitized. When side scan features were unclear due to navigational challenges experienced during collection, we used our best judgement to identify the boundaries of a SAV area. Finally, those SAV features occurring adjacent to the bank were

snapped to a bankwidth polygon layer created from Google Earth imagery collected almost contemporaneously to our study period (03/2017 and 05/2017).

2.4.2. Tules and Cattails

Due to the documented association of many Delta fish species with areas of vegetation (Moyle 2002), we included a metric specific to tules and cattails, as these areas of three-dimensional habitat may provide cover for ambush predators. We utilized the existing delta vegetation dataset (available for download https://www.wildlife.ca.gov/Data/GIS/Vegetation-Data), and selected for species of Cattails and Tules (*Schoenoplectus spp.* and *Typha spp.*) in order to describe the location and area of these regions within our study areas.

2.4.3. Artificial structures and Levees

The Sacramento-San Joaquin Delta is dominated by artificial structures, especially large water diversions and rip-rapped levees, both of which alter hydrodynamic conditions locally, and may facilitate the persistence of non-native fish species (Feyrer and Healey 2003). To define the presence and areal coverage of artificial structures within our study sites, and in turn include these measures as factors in our models, we used the Passage Assessment Database (https://nrm.dfg.ca.gov/PAD/) to define the position of diversions. We then mapped these features, as well as any other man-made structure from Google Earth Imagery (imagery dates 03/2017-05/2017). These features were hand-digitized in Google Earth, sometimes utilizing historical imagery to estimate area of features, and then brought into ArcGIS. In addition to prominent man-made features, we included a metric for the presence of levees within our study sites, as Chinook salmon tend to prefer natural bank types to rip-rapped ones (Garland et al. 2002). We included a parameter for the location of levees within 50 m of a given study site, utilizing the National Levee Database (http://nld.usace.army.mil/egis/f?p=471:1).

2.4.4. Depth and pools

Depth is another important physical feature for assessing the availability of fish habitat in riverine systems (US EPA 2009). Deep water pools may provide shelter for predator species, thus increasing predation risk for Chinook smolts within these zones. Unlike riverine pools and riffles, however, in many cases these deep pools are simply areas of relatively deeper bathymetry with similar water velocities as adjacent stretches of the waterway. To describe pool habitat for our study regions, we utilized the San Francisco Bay-Delta digital elevation model developed by USGS (Fregoso et al. 2017), a 10 m x 10 m bathymetry layer covering the extent of our study area. For each site, we clipped the bathymetry layer to within our bank line for each study site, and calculated the mean depth and standard deviation of depth values for each site. We then selected only those pixel values whose depth value was deeper than 1.5 standard deviation from the mean depth for a given site. By then converting these pixel values into polygon features, we were able to calculate the total area of pool habitat per site, and estimate the proximity of a predation event to a given pool feature.

2.4.5. Bottom slope, bottom roughness, and sinuosity

Habitat complexity can be an important predictor of predators habitat use and predation success. To quantify habitat complexity, sinuosity, bottom slope, and bottom roughness (standard deviation of depth [Grant and Madsen 1986]) were estimated. We estimated bottom slope and bottom roughness from the USGS bathymetry layer, both of which describe bottom heterogeneity, which in turn may

influence the suitability of the river bottom as predator habitat. Bottom slope represents the angle (0º to 90º degrees) from horizontal between adjacent depth readings. Sinuosity values were calculated as the distance the water travels within a study site polygon, divided by the Euclidean length for that site. Sinuosity can also be a strong predictor of habitat complexity and variability in water velocities, and in turn can influence the propensity of fish (and likely piscine predators) to use that habitat (Roni et al. 2014).

2.4.6. *Distance from shore*

Distance from shore can also be an important factor in determining habitat complexity in the Sacramento-San Joaquin Delta. The vast majority of the Delta is channelized and leveed. In many places, only the margins of the river allow for shallow-water habitat and vegetation growth. Furthermore, the rip-rap rocks, used for levee stabilization, are often the only rock habitat that exists in parts of the Delta, the rest being mud and sand bottom. Finally, two of the most important salmon predators in the Delta, striped bass and largemouth bass, are numerically dominant in distinct parts of the cross-sections of the waterways: striped bass are numerically dominant in the river channel areas, while largemouth bass are numerically dominant in the littoral margins (Michel et al. 2018).

2.4.7. *Flow velocity*

Flow velocity can have an important influence on predator distribution as well as ability of prey to evade capture (reviewed by Čada et al. 1997). We used PER speed over ground as a surrogate for flow velocity since PERs drift with the surface current and are negligibly affected by other forces (such as wind).

2.4.8. *Turbidity and light*

Turbidity and light level are both considered important predictors of predation by piscine predators. When turbidity is high, or light levels are low, predator efficiency decreases, especially for predators that use sight as a primary means of prey detection (Gregory and Levings 1998, Sweka and Hartman 2003). Light level may also represent cloud cover and time of day, which can both have important impacts on predator activity (reviewed by Helfman 1986).

2.4.9. *Conductivity*

The salinity tolerances and preferences of the primary piscine predators of the South Delta differ considerably (Moyle 2002). Notably, striped bass will make frequent incursions into seawater environments, while largemouth bass will not. Therefore, we included conductivity as a potentially important environmental variable.

2.4.10. *Water temperature*

Finally, water temperature can be an important determinant of predation risk on at least two important levels. Firstly, seasonal patterns of fish migration can be triggered by temperature changes, such as with striped bass (Callihan et al. 2014). Secondly, water temperature directly influences metabolic activity of fish, and therefore, energy demands. All else being equal, increases in water temperature should increase predator activity and foraging.

2.5. *Predator distribution, abundance and density using DIDSON cameras*

Concurrently with PER sampling, a separate boat and crew collected information on the distribution, abundance and density of predators within the same site using DIDSON cameras. We used two boat-mounted DIDSON units simultaneously to survey potential salmon predators. The cameras were affixed to opposite sides (port and starboard) of an 18 foot aluminum jet boat using adjustable pole mounts. Like all acoustic equipment, DIDSONs gather information on the environment by transmitting a sound wave and processing the returning sound. To avoid acoustic noise created by cross-communication between the two DIDSONs, we aimed the cameras in opposite directions (pers. comm. Sound Metrics staff, 2017). By aiming the DIDSONs perpendicular to the vessel, which was surveying parallel to the length of the channel, we were able to generate broad fields of view for the cameras, focused on both littoral and mid-channel habitats. This orientation also had the benefit of generally ensonifying targets perpendicular to the DIDSON beam, to provide the best target resolution (Tuser et al. 2014, Hightower et al 2013, Hateley and Gregory 2005).

The adjustable pole mounts allowed for fine-tuning of the pan, tilt, and height of the DIDSON units (Cronkite and Enzenhofer, 2005). We set the pole mounts to a height of 1 meter below the gunnel, putting the DIDSON approximately 30 cm below the surface of the water. We set the DIDSONs' window lengths (the maximum window length in high frequency mode) to 10 meters with a window start of 2.08 meters from the lens to maximize the viewing range and exclude areas immediately adjacent to the survey vessel. To maximize correspondence with concurrent PER observations, we tilted the DIDSONs approximately 10 degrees downward from horizontal to capture the upper water column just below the water's surface with minimal interference from the surface. We fixed panning at 90 degrees from the direction of travel.

Within each 1 km survey reach, DIDSON surveys followed longitudinal transects. Depending on the shape of the survey reach, we utilized different transect methods to ensure transects adequately covered the reach. Given the survey vessel was 2.5 meters wide and the DIDSON settings allowed for a 12.08 meter viewing range (2.08 meter window start + 10 meter window length) on both sides of the vessel (Fig. 3). We offset transects approximately 12 meters from either the shore, or the edge of the survey area, and sites that were less than 90 meters wide were surveyed by two longitudinal transects to avoid overlapping the survey areas of adjacent transects. At sites 90 meters wide or greater, we conducted one or more mid-channel transects in addition to the shore transects. At sites with channel widths varying along the length of the reach, we used a hybrid of the two approaches to cover the area surveyed by the PERs. We repeated transects throughout the evening survey period during the last two hours of daylight and the first hour after sunset when predator and prey activity are typically high (Demetras et al. 2016).
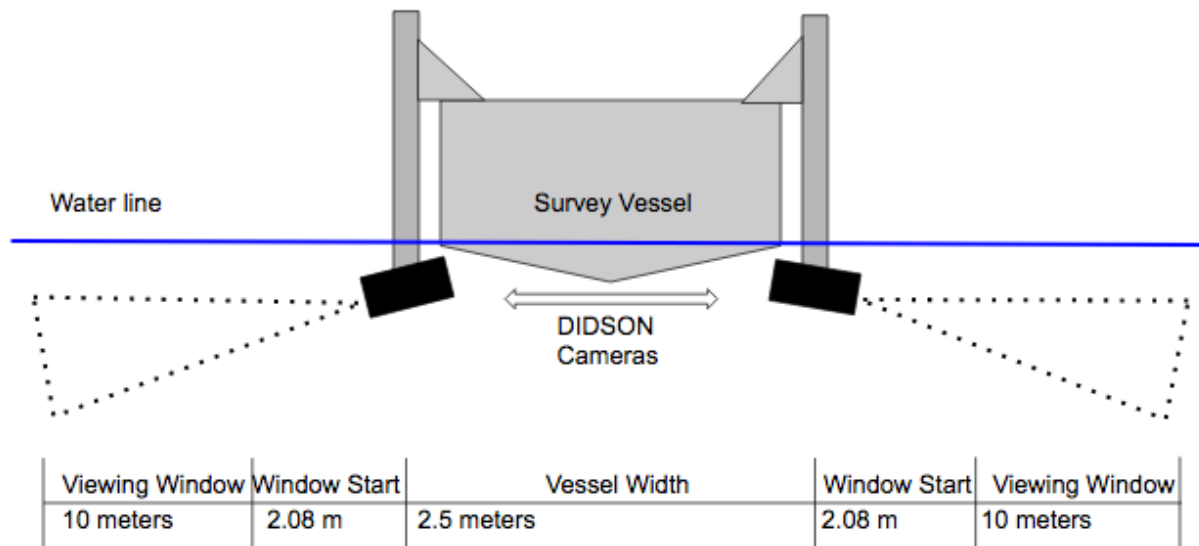
Viewing Window	Window Start	Vessel Width	Window Start	Viewing Window
10 meters	2.08 m	2.5 meters	2.08 m	10 meters

Figure 3: Survey vessel setup. Distances are not drawn to scale.

During surveys, the boat was powered by an electric trolling motor to avoid disturbing target fish along the transect and to fine-tune the survey speed. We performed surveys at a rate of approximately 2 km/h and we closely monitored speed via a Garmin GPS device installed on the survey vessel. This survey speed was chosen to optimize video resolution while also maximizing the number of transects performed per survey. At 2 km/h, a single transect took approximately 30 minutes to survey, theoretically allowing for approximately six 1-km transects within the 3-hour survey window; however, poor survey conditions and technical difficulties at times resulted in fewer transects.

Transect paths were recorded by GlobalSat USB GPS receivers linked to each DIDSON. The DIDSONs recorded the GPS positions for each acoustic frame along the transect, allowing predators identified using the DIDSON cameras to be assigned to a specific location.

2.6. DIDSON Estimates of Predator Density and Abundance per reach

We derived an average predator density for each reach from the DIDSON transects. We surveyed reaches in a non-random, systematic order to maximize survey area coverage. We attempted to replicate transects to increase the resolution of density estimates; however, transects were not always replicated due to constraints of field conditions, equipment malfunctions and site variability. To account for this variability, we first estimated densities per transect, and reach density was then estimated as the bootstrapped mean of all the transect densities.

Prior to density calculations, we weighted each predator observation as a function of its range from the DIDSON camera. Because the viewing area, or arc length, of the survey window increases proportionally with range (arc length = radius x angle), we had more area to view fish at farther ranges. Conversely, at closer ranges there was proportionally less area to observe associated predators. Thus, we weighted observed predators by the ratio of maximum survey window range (R_{max}) to the observed

predator range (*i*) to account for the change in viewing area. Since the angle of the viewing window is constant, it was not necessary to include it in the function. The weight of a predator fish at the observed range (*wᵢ*) was calculated as follows:

$$(3) \quad w_i = e^{(R_{max} - R_i)/R_{max}}$$

where R_{max} is the maximum viewing range for the transect and R_i is the range of the observed range of a predator fish. As the observed range approaches the maximum range, the weight approaches 1. A predator fish observed in the near field, e.g. R_i = 2 meters when R_{max} = 12 meters, would receive a weighting of approximately 2.29. We tested this weighting function with simulations using the WiSP R package (Zucchini et al. 2007) and we found that it generated accurate estimates of the true abundance and was robust to a variety of fish distributions and densities.

We calculated the density of predator fish in each reach (*Dⱼ*) using independent subsets of transect (i.e. non overlapping survey efforts) with the following equation:

$$(4) \quad D_j = \frac{\overline{p_j}}{\overline{a_j}}$$

where $\overline{p_j}$ is the mean number of predators observed per transect *j* and $\overline{a_j}$ is the mean area surveyed per transect. Area surveyed per transect was calculated as the sum of the product of window length and transect length for each DIDSON operated.

To account for repeatedly surveyed areas while utilizing all of the available data, we constructed a bootstrap distribution of predator densities for each reach. Using all possible independent subsets of two or more transects, we calculated a density using equation 4. The mean and variance of the resulting distribution of densities was used as the final reach density and associated variance term.

2.7. Estimation of fine-scale predator distributions within each reach

In order to provide an index of predator abundance with high spatial and temporal resolution for each PER data point, we used a nearest neighbor analysis with a time-scaled distance measure between all observed predators and each PER within a sample reach. A time-scaled distance (D_{ij}) between two points i and j was calculated following the same practice used in t-LoCoH home-range construction (Lyons et al. 2013) summarized in the equation below:

$$(5) \quad D_{ij} = \sqrt{\Delta x_{ij}^2 + \Delta y_{ij}^2 + (s \times y_{max} \times \Delta t_{ij})^2}$$

where *s* is a dimensionless scalar to control the effect of time and y_{max} is the maximum velocity of a predator fish. For this analysis, we set y_{max} equal to the maximum swimming velocity of a striped bass, 0.83 m/sec (Freadman 1979). *S* was selected to produce nearest neighbor sets composed of

approximately 50% time-selected predators, ensuring that the final metric incorporated predators that were known exist near a PER both in time and space. For this analysis, s was set to 0.03.

For each PER location, we calculated the time-scaled distance from the PER to all observed predators in a sample reach ("mean predator distance"). We then selected the nearest 10 predators and the true distance between these predators and the PER was calculated. We used the mean of those 10 distances as the final index of local predator abundance. If a PER location was greater than 1 meter from any surveyed area, we excluded it from the analysis.

2.8. Predator Density Model

To identify the environmental factors influencing the distribution of predator fish across the study region, we modeled reach predator density using linear mixed effects regression. We chose a set of candidate predictors variables from the compiled data for the study region based on their hypothesized influence on predator distribution. We then scaled all area-dependent variables by area of their respective study reach. We then standardized all continuous variables by subtracting the means and dividing by the standard deviation. We also log-transformed predator densities to fit a log-normal distribution. Prior to model fitting, we conducted pairwise correlations to assess collinearity and removed a single covariate from any pair with a correlation greater than 0.7.

The linear predictor variables were:
- Flow velocity, as estimated from local PER speeds (m/sec)
- Turbidity (NTU)
- Conductivity (mCsm)
- Temperature (ºC)
- Submerged aquatic vegetation (area [m^2] and patch count)
- Tule vegetation (area [m^2] and patch count)
- Man-made structures (area [m^2] and count)
- Sinuosity
- Levees (length along the channel [m])

We used Akaike's Information Criterion corrected for small sample size (AICc) to select the most parsimonious model based on both the random and fixed effects structure (Akaike 1974). To account for the repeated measures of the repeat sites, we used a random intercept for week in all candidate models. We also used random intercepts for site area, region, and average depth as these variables introduced random variation that was not controlled in the survey methodology. After a mixed effects structure was chosen, we performed model selection on all possible subsets of four or less predictor variables and ranked models based on their respective AICc scores. We assumed models with ΔAICc < 2 had equal support (Burnham and Anderson 2002); thus, if multiple models had a ΔAICc < 2, we selected the one with the fewest parameters, i.e. the most parsimonious model.

2.9. Seasonal Trends Predation Risk Model

To understand the underlying week-over-week seasonal trends in predation risk, we visited three of the study sites repeatedly for all six consecutive weeks of the study (repeat sites 01, 25, 28). We subset the PER data for this exercise to only include data from those repeat sites, for a total of 18 sampling days. We collected a suite of environmental and habitat variables that were believed *a priori* to have a potential influence on seasonal trends in predation risk and summarized them, where applicable, to the median value for that sampling day at that site. We then standardized those daily median values, allowing for the comparison of beta parameter estimate importance.

The linear predictor variables were:
- Turbidity (NTU)
- Conductivity (µScm)
- Temperature (Celsius)
- Light (Lux)
- Predator Density (predators/$10m^2$)
- PER Speed (m/sec, a proxy for water velocity)
- PER deployment time (to account for unequal deployment time – there is a presumed increased risk with longer deployment times)

And factor:
- Site (to account for differences in inherent site predation risk)

For a total of 256 distinct models.

To test for seasonal changes in predation risk, we selected a logistic regression model, with whether a PER was predated upon (1) or not (0) as the binary response variable. We created and tested model fit for a suite of models with all possible combinations of the predictor variables using the dredge function in R (Kamil Barton (2018). MuMIn: Multi-Model Inference. R package version 1.42.1. https://CRAN.R-project.org/package=MuMI) in R statistical software, vers. 3.3.0 (R Core Team, 2016). We selected the most appropriate model by examining the difference in AICc values between each model and the model with the lowest AICc (**ΔAIC**).

2.10. Fine-scale spatial-temporal Predation Risk Model

In order to determine fine-scale spatial and temporal relationships between habitat and water quality variables and predation risk, we choose to use a Cox proportional hazards model for the second analysis. The Cox proportional hazard model (Cox 1972, Therneau and Grambsch 2000) is a time-to-event model that estimates the instantaneous rate of an event, in this case predation, as a function of predictor variables. The response variables for a Cox model are the right-censored time interval length and whether an event (predation) occurred during that interval. The measure of an effect in a Cox model is the hazard ratio. Hazard ratios between 0 and 1 mean that the risk is decreased, specifically divided by that amount, i.e. a predation hazard ratio of 0.5 means that predation risk will be reduced by half. A

hazard ratio of 1 means risk remains unchanged. A hazard ratio above 1 means that risk is increased, specifically multiplied by that amount, i.e. a predation hazard ratio of 2 means that predation risk will be doubled.

For this exercise, we used data from all single-visit study sites, as well as data from only one visit per repeat site. We objectively selected the repeat site visit given the GRTS selection order. For example, for repeat site 25, only the sixth visit to this site on May 8th was used because it was the first visit that occurred after the single-visit site 24 was visited on May 5th. In total, data from 20 study sites were used, from 20 distinct sampling days.

The PERs record their GPS coordinates every 3 seconds. However, most environmental variables fluctuate at longer time scales. Furthermore, allowing for longer time intervals decreases model processing time, and therefore we thinned the data to one record per minute of PER deployment time. We associated a suite of environmental and habitat variables that were believed *a priori* to have a potential influence on high-resolution spatial-temporal patterns in predation risk to the PER data at the one minute intervals. We then performed pairwise comparisons of continuous variables to determine if any variables were collinear (Supplemental Fig. 1) using the corrplot package in R (Taiyun Wei and Viliam Simko (2017). R package "corrplot": Visualization of a Correlation Matrix (Version 0.84). https://github.com/taiyun/corrplot). If any variables had correlation coefficients above 0.7, we used previous published studies to inform which of the two variables were retained for the analysis.

Prior to fitting the Cox models, we standardized covariate values such that the resulting standardized beta coefficients could be interpreted as the predicted change in the hazard ratio given a one standard deviation increase in the covariate value. This also allowed for an easier comparison between different covariate impact parameter estimates.

The linear predictor variables were:
- Turbidity (NTU)
- Conductivity (μScm)
- Temperature (Celsius)
- Light (Lux)
- PER Speed (m/sec, a proxy for water velocity)
- Depth (m)
- Bottom slope (incline in degrees)
- Pools (binary, 1 if point was in pool, 0 otherwise)
- Submerged Aquatic Vegetation ("SAV"; binary, 1 if point fell within 3 meters of SAV, 0 otherwise)
- Distance from shore (m)
- Mean Predator Distance (m)
- Sinuosity
- Standard Deviation of Depth

One *a priori* non-linear predictor variable was also included:
- Time to sunset (minutes, values before sunset negative, after sunset positive)

One random effect was also included
- Site (to account for inherent differences in site predation risk)

We created and tested model fit for a suite of Cox proportional hazard models with all possible combinations of the predictor variables, using the dredge function in R and run using the Surv, coxph and pspline functions from the "survival" package in R (vers. 2.38, Therneau T (2015). A Package for Survival Analysis in S. version 2.38, https://CRAN.R-project.org/package=survival). We used the pspline function to allow time to sunset to have a penalized spline (non-linear) basis, with 4 degrees of freedom. This was decided *a priori* because previous studies have indicated that maximum predation risk occurs near sunset, with decreases in predation risk before and after. No other predictor variables were allowed to have non-linear relationships with predation risk.

We again selected the most appropriate model by examining the difference in AICc values between each model and the model with the lowest AICc (**Δ**AIC).

2.11. South Delta-wide extrapolation of Predation Risk Model

Future applications of this and similar projects will likely be focused on extrapolating the statistical relationships found here to spatial and temporal scales more relevant to the management of prey species. As such, we made preliminary efforts into extrapolating our most parsimonious Predation Risk Model to the entire South Delta, from Mossdale to Jersey Point on the lower San Joaquin River including all major sloughs and waterways adjoining the Lower San Joaquin River on its river-left side. Because the statistical relationships found in the Predation Risk Model are based off of data collected in rivers and sloughs only, we did not attempt to extrapolate Predation Risk to large open bodies of water in the South Delta, such as Franks Tract and Mildred Island.

The extrapolation was performed by first dividing the sloughs and rivers of the South Delta into approximately 1-km long segments along the thalweg of those waterways, resulting in a total of 309 1-km segments. We then collected and summarized the habitat variables that occurred in the most parsimonious Predation Risk Model per 1-km segment. We then selected the temporally fluctuating variables from the most parsimonious model and simulated data values along their ranges of observed values. We then used these habitat and temporal variables to predict Predation Hazard Ratios for each 1 km segment given the parameter estimates in the most parsimonious model. In the situation that mean predator distance was a predictor in the most parsimonious model, we used predator densities as estimated by the Predator Density Model as a proxy. We would first generate predator densities for the same 1-km segments throughout the South Delta. To then convert those values to mean predator distances, we assumed uniform distribution of predators. Given that, we can use the following equation to find the mean predator distance for the 8 nearest neighbors.

$$(6) \quad \frac{\left(4 \times \sqrt{\frac{1}{D_r}}\right) + \left(4 \times \sqrt{\frac{1}{D_r} + \frac{1}{D_r}}\right)}{8}$$

where D_r is the predicted reach density in predator/m^2. The first term of the numerator is the distance in meters from the 4 closest predators, at the N, S, E, and W (perpendicular) bearings. The

second term is the next 4 closest predators, at the NW, NE, SW, and SE (diagonal) bearings. The mean predator distance used in the Predation Risk Model was the mean of the 10 nearest predators, however estimating this, even given uniform distribution of predators, would be substantially more computationally complex (but will be attempted in subsequent analyses). For the purposes of this analysis, Equation 6 produced a reasonable approximation for mean predator distance based on results from a linear model between the empirically estimated mean predator distances and the approximated mean predator distances ($r^2 = 0.5$).

3. Results

3.1. PER summary statistics

After assessing selected sites for proximity to other selected sites (using the 3 river km cutoff), we dropped 15 sites and replaced them with the next 15 oversampled sites from the GRTS draw. Furthermore, we dropped one site in the middle of Frank's Tract on the day of sampling due to the large wind waves making PER deployment logistically difficult (and we replaced it on the same day with a nearby oversampled site). We also dropped one sampling day from the schedule due to a river otter breaking into the livewell and eating Chinook salmon smolts that were to be used for baiting the PERs that evening.

In total, we visited 20 unique sites starting April 3rd and ending May 13th of 2017, three of which were repeat sites that we visited every week for 6 weeks (Supplemental Table 1). The repeat sites were located in the Upper San Joaquin River region, in the Turner Cut region, and in the Lower San Joaquin Region [sites 25, 28 and 01, respectively (Fig. 4)]. In total, we deployed 1,670 PERs during the spring of 2017, of which 15.7% were predated on.
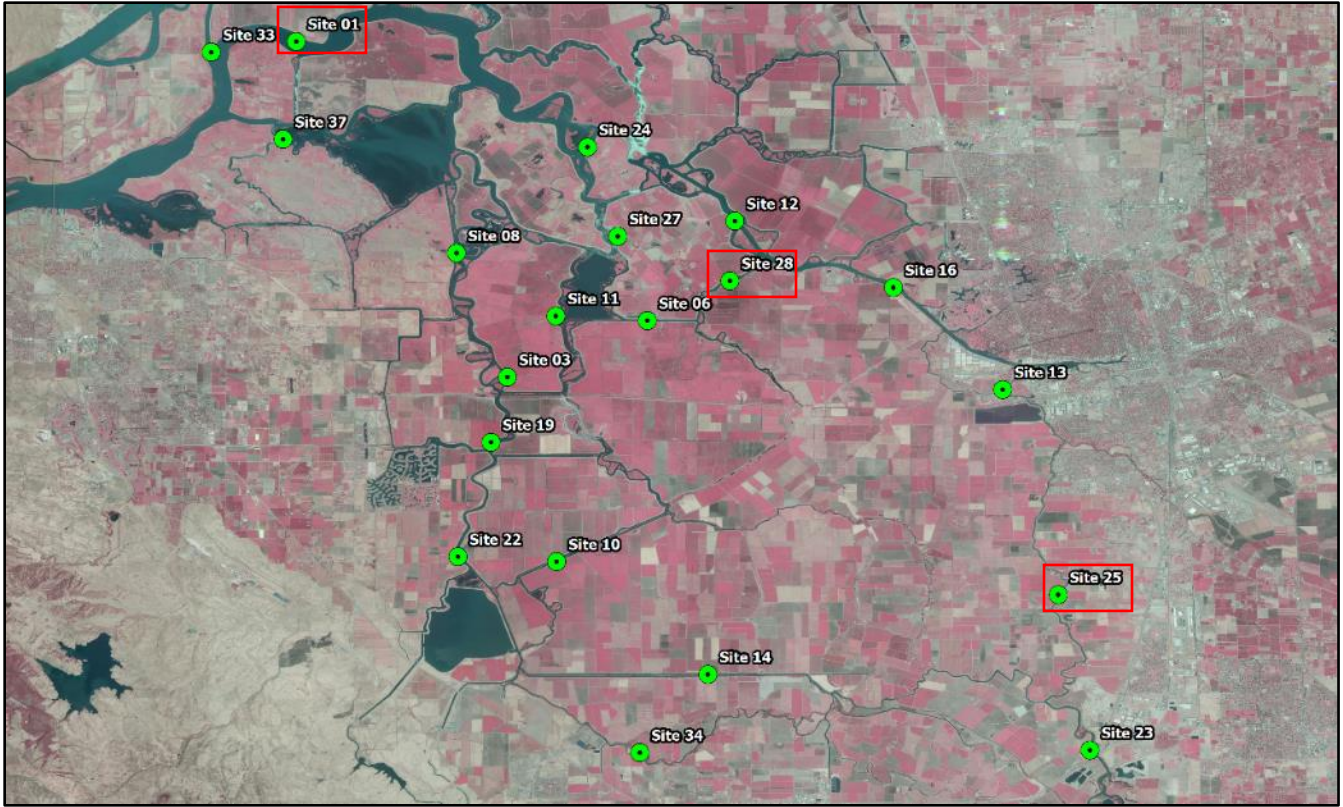
Figure 4. Map locations of the final sites visited during the 2017 study. Refer to Supplemental Table 1 for more information on each site. Repeat sites are highlighted with a red box.

3.2. Temporal patterns in predation

Overall, conditions in the South Delta in the spring of 2017 were abnormal. River flows were high after a historically wet winter, with some zones of the Delta having water levels almost overtopping the levees. Percent of predated PERs varied through time and between sites, ranging from 0 to 37% (Supplemental Table 1 and Fig. 5). Overall, there was an increasing trend in percent of predated PER as the season progressed (Fig. 5).

Three PERs floating through Turner Cut (left); crew on the small boat "Heron" recovering a PER from the lower San Joaquin River region (E. Danner).
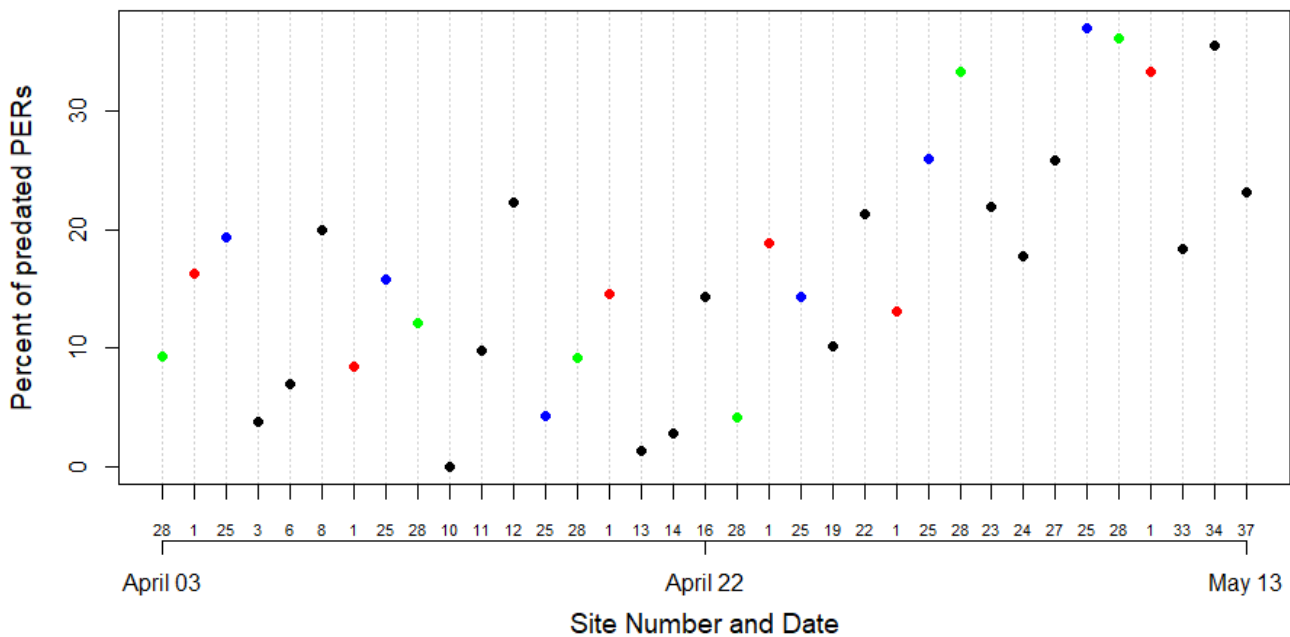
Figure 5. Percent of predated PERs through time during the 2017 field season. The x-axis has both sample site number (above) and date (below). Black points depict sites visited only once, colored points depict repeat sites (site 1 in red, site 25 in blue, and site 28 in green).

Weekly predation rates at the repeat sites also indicated a general increasing trend in predation rates through the field season. Week 6 had significantly higher predation rates than weeks 1 through 4 (Fig. 6).
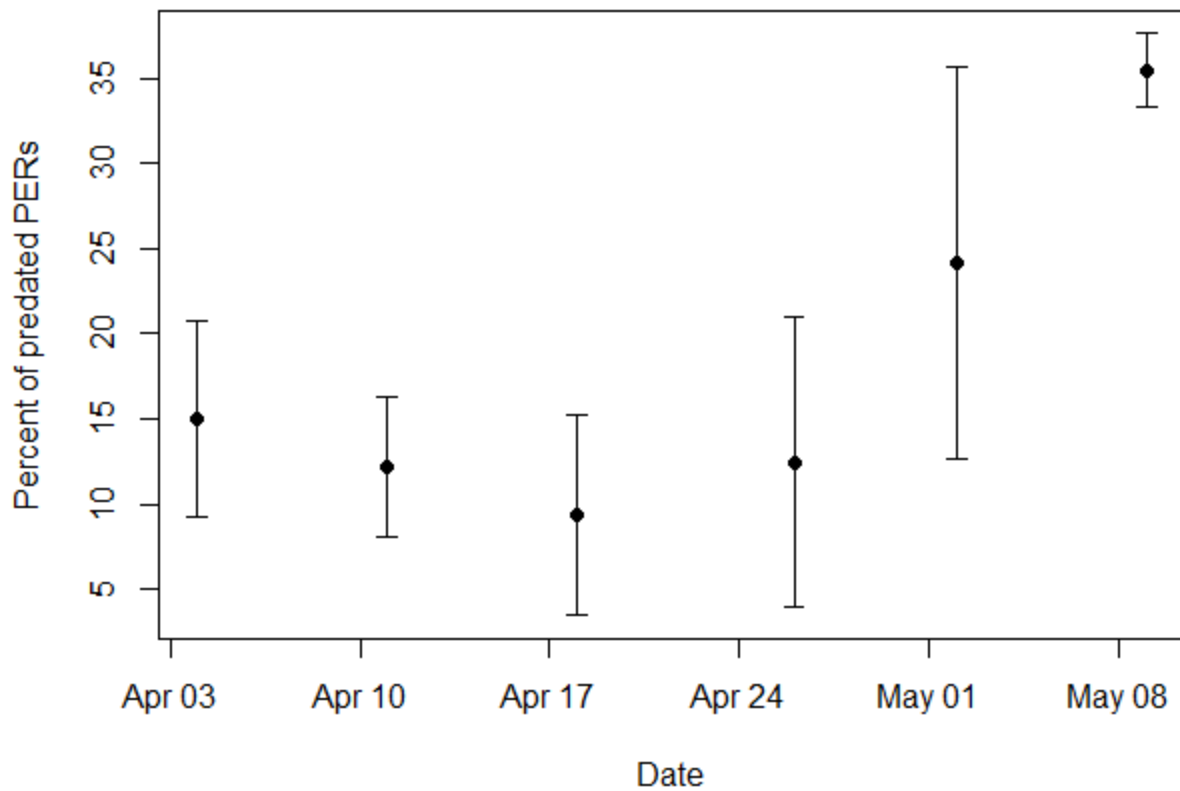
Figure 6. Mean weekly percent of predated PERs at repeat sites only (with 95% confidence intervals) through time.

3.3. Spatial patterns in predation

Regional predation rates showed no significant differences (Fig. 7). The Franks Tract, Middle San Joaquin River, and Upper Old River regions had too few sites to accurately estimate confidence intervals.
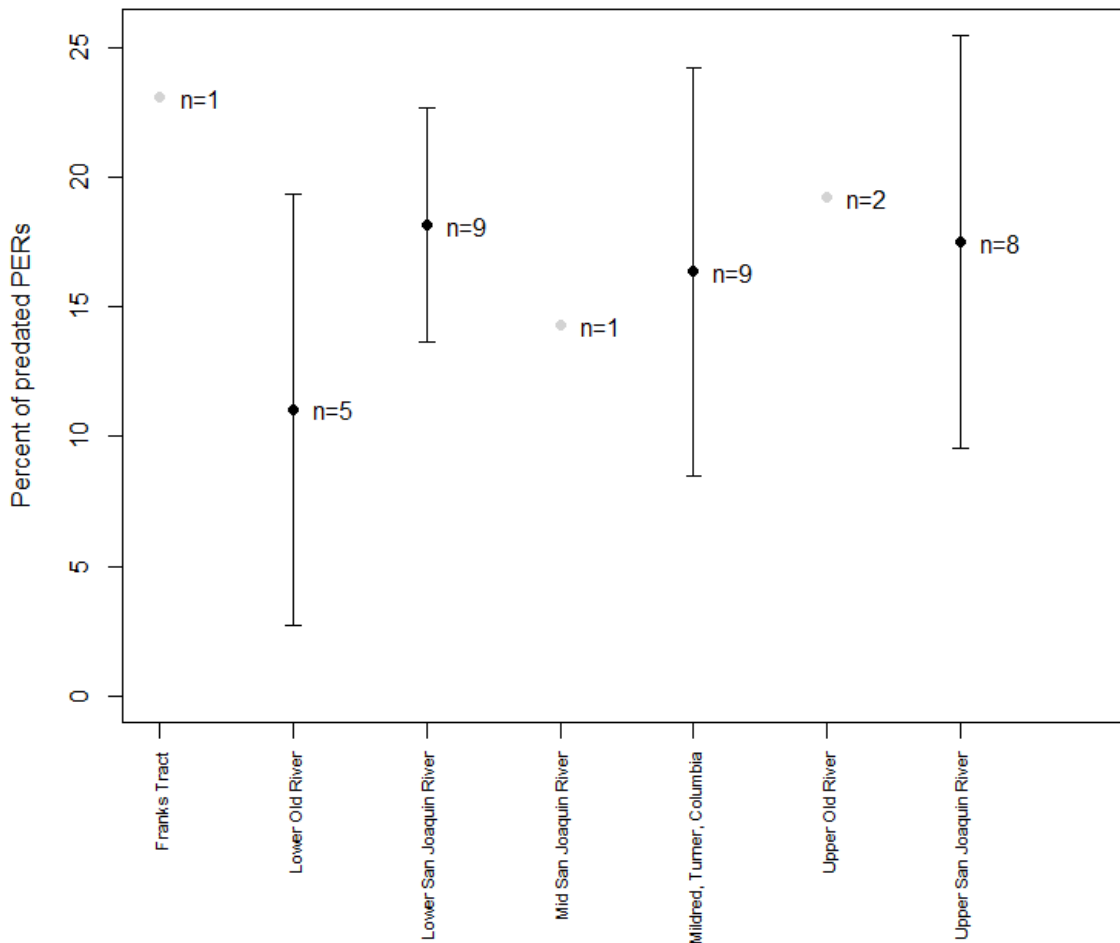
Figure 7. Mean percent of predated PERs per GRTS region, with 95% confidence intervals. Number of sites visited within each region is shown near each data point. If less than 3 sample sites were visited per region, confidence intevals could not be accurately estimated and the point estimate was depicted in grey.

3.4. Habitat features

We deployed a water quality sonde in every field site before PER deployments began. This sonde recorded temperature, conductivity, and turbidity at one minute intervals. Habitat data was successfully collected and georeferenced for all 20 sites. These included:

- River depth (meters)
- Pools (derived from river depth)
- Leveed shoreline
- Submerged aquatic vegetation
- Manmade structures in river
- Tree canopy over water

- Sinuosity
- Channel type
- Tules

To demonstrate the current geographic resolution and distribution of predation events (from PERs), predators (from DIDSON scans) and habitat features, we generated maps depicting these datasets for the repeat sites 01, 25 and 28 (Supplemental Figs. 2,3,4).

3.5. Predator abundance and densities

Estimates of predator abundances and density show large variability between sites and through time (Fig. 8). Reach abundances varied from 29 to 1,640 predators, and reach predator density varied from 0.07 to 0.57 predators per $10m^2$ (Supplemental Table 2).
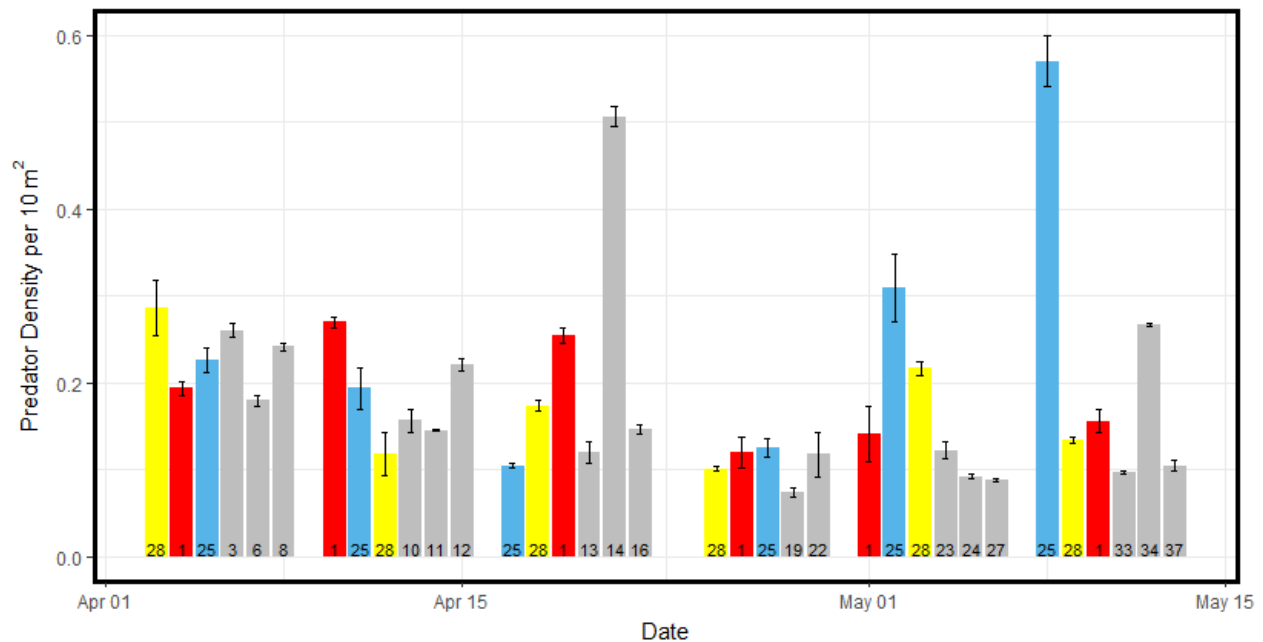

Figure 8: Predator densities (predators per $10m^2$) per site, ordered chronologically, with 95% confidence intervals (± 1.96 SE). Grey bars depict sites visited only once, colored bars depict repeat sites (site 01 in red, site 25 in blue, and site 28 in yellow). Numbers within bars are site numbers.

3.6. Predator Density Model

The best mixed effects model structure for the landscape-scale predator distribution model included both a random intercept for week and a random intercept for average depth. Model selection resulted in

three models that were within a **ΔAICc** of 2 (Table 1). Sinuosity and SAV patch count were present in all three of these models and a model using only those two variables received the highest support based on AICc scores. This model was thus chosen as the final model of predator distribution.

Table 1: Model selection results for landscape-scale predator distribution (only models with ΔAICc of 2 or less are shown). The most parsimonious model is highlighted in red. Greyed out boxes depict covariates that were not included in that particular model.

Intercept	SAV area	SAV patch count	Sinuosity	Tule Count	Adjusted R²	Degrees of Fredom	AICc	ΔAICc	weight
-6.41		0.28	-0.19		0.35	6	51.03	0	0.06
-6.41		0.32	-0.22	0.12	0.43	7	51.53	0.50	0.05
-6.41	0.12	0.36	-0.25		0.41	7	52.00	0.97	0.04

3.7. Seasonal trends in Predation Risk Model

The most parsimonious logistic regression model that described the seasonal patterns in predation risk in the South Delta in the Spring of 2017 included light level and temperature (Table 2). Model selection resulted in 11 models that were within a **ΔAICc** of 2. Both light level and temperature were estimated to have a positive relationship with predation risk (Fig. 9), with temperature having the stronger relationship.

Table 2: Model selection results for seasonal predation risk (only models with ΔAICc of 2 or less are shown). The most parsimonious model is highlighted in red. Greyed out boxes depict covariates that were not included in that particular model.

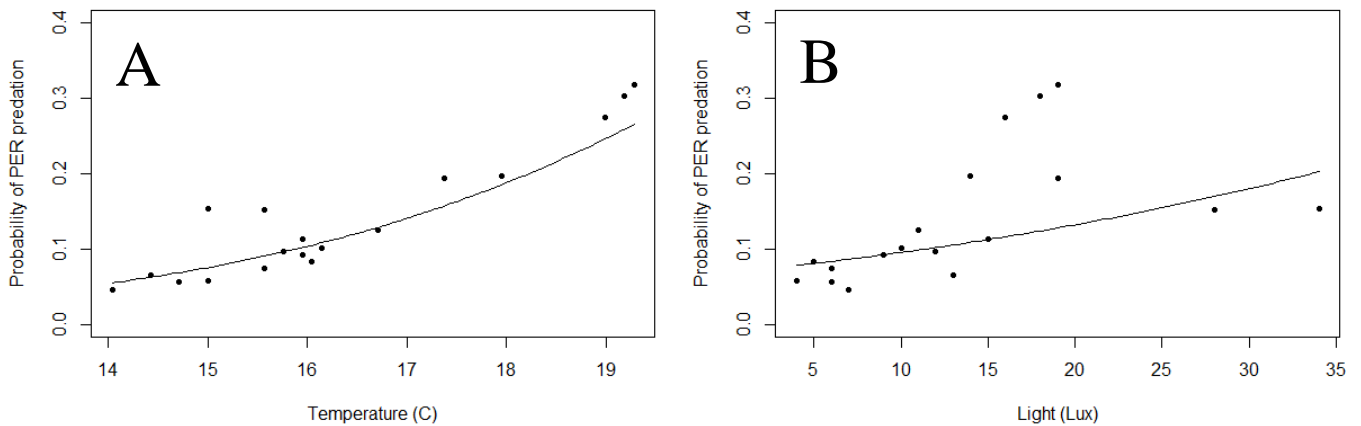| Intercept	Conductivity	Light	Predator Density	Temperature	PER Speed	Deployment Time	Turbidity	Site	# of Parameters	ΔAICc
-2.03		0.29		0.53		-0.20			4	0.00
-2.04		0.25		0.57			0.22		4	0.39
-2.03		0.27	0.16	0.52					4	0.41
-2.02		**0.29**		**0.53**					**3**	**0.70**
-2.04		0.27	0.11	0.52		-0.15			5	1.03
-2.04		0.26		0.55		-0.15	0.14		5	1.26
-2.03		0.30		0.55	0.14				4	1.39
-2.04		0.24	0.11	0.54			0.15		5	1.54
-2.01				0.63			0.27		3	1.68
-2.03		0.29		0.53	0.04	-0.18			5	1.93
-2.03	-0.05	0.28		0.53		-0.20			5	1.93

Figure 9: Simulated relationship between (A) temperature and (B) light level and the probability of PER predation, given parameter estimates from the most parsimonious Season Predation Risk model. Empirical data are overlaid as points.

3.8. Fine-scale spatial-temporal Predation Risk Model

The most parsimonious Cox proportional hazard model which describes the fine-scale spatial and temporal patterns in predation risk in the South Delta in the Spring of 2017 includes temperature, sinuosity, mean predator distance, and time to sunset (Table 3). We ran a total of 16,383 models, of which 23 models were within a ΔAICc of 2 from the lowest AICc score. Predicted PER survival proportion through time decreased to approximately 0.8 (or 0.2 PER mortality) over the span of 5000 seconds (83.3 minutes) (Fig. 10). Both temperature and sinuosity were estimated to have a positive relationship with predation risk, while mean predator distance had a negative relationship with predation risk (Fig. 11). Time to sunset had a strong nonlinear relationship with predation risk, such that maximum predation risk (a three-fold increase over average conditions) occurred approximately 40 minutes after sunset.
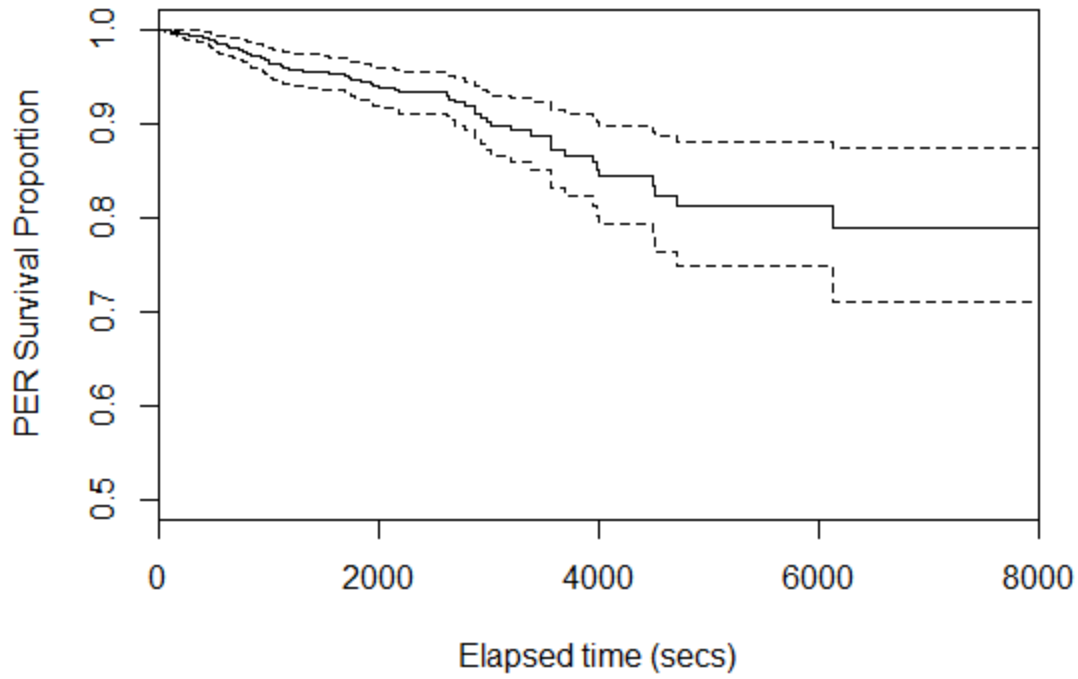
Figure 10: Predicted PER survival proportion through time from most parsimonious Cox Proportional Hazard model. Solid line represents the PER survival proportion at a given time (secs), while the dashed lines represent the 95% confidence limits above and below this line.

Pools	Time to sunset	SAV	Mean predator distance	Conductivity	Depth	Distance to shore	Light	SD of Depth	Sinuosity	Bottom Slope	Temperature	PER speed	Turbidity	# of Parameters	ΔAICc
	+	-0.65	-0.55	-0.29				0.23	0.39		0.34	-0.34		11	0.00
	+	-0.62	-0.54						0.23		0.50			8	0.38
	+	-0.60	-0.56					0.19	0.25		0.50			9	0.42
	+	-0.67	-0.54	-0.27					0.36		0.35	-0.30		10	0.68
	+		-0.57	-0.31				0.24	0.38		0.30	-0.28		10	0.75
	+		-0.58					0.21	0.26		0.47			8	0.89
0.59	+		-0.57	-0.30				0.26	0.36		0.29	-0.31		11	0.89
0.50	+	-0.59	-0.55	-0.29				0.26	0.37		0.33	-0.35		12	0.91
0.57	+		-0.57					0.22	0.23		0.46			9	0.98
	+		-0.56						0.25		0.47			7	1.28
0.48	+	-0.53	-0.55					0.21	0.23		0.49			10	1.31
	+	-0.71	-0.53						0.31		0.48	-0.17		9	1.45
	+	-0.69	-0.55					0.20	0.33		0.47	-0.18		10	1.46
	+		-0.57	-0.18				0.21	0.26		0.40			9	1.48
0.39	+	-0.57	-0.53						0.22		0.49			9	1.70
	+	-0.54	-0.55	-0.15				0.20	0.25		0.44			10	1.79
0.50	+		-0.55						0.22		0.46			8	1.85
	+		-0.56	-0.29					0.35		0.31	-0.25		9	1.86
	+	-0.63	-0.54						0.24	0.12	0.51			9	1.89
	+		-0.60	-0.33	0.21				0.38		0.29	-0.28		10	1.92
	+	-0.58	-0.54	-0.13					0.23		0.45			9	1.92
	+		-0.55					0.23	0.24		0.49		0.10	9	1.93
	+	-0.56	-0.54					0.21	0.23		0.51		0.09	10	1.93

Table 3. Model selection results for fine-scale spatial-temporal predation risk (only models with ΔAICc of 2 or less are shown). The most parsimonious model is highlighted in red. Greyed out boxes depict covariates that were not included in that particular model.
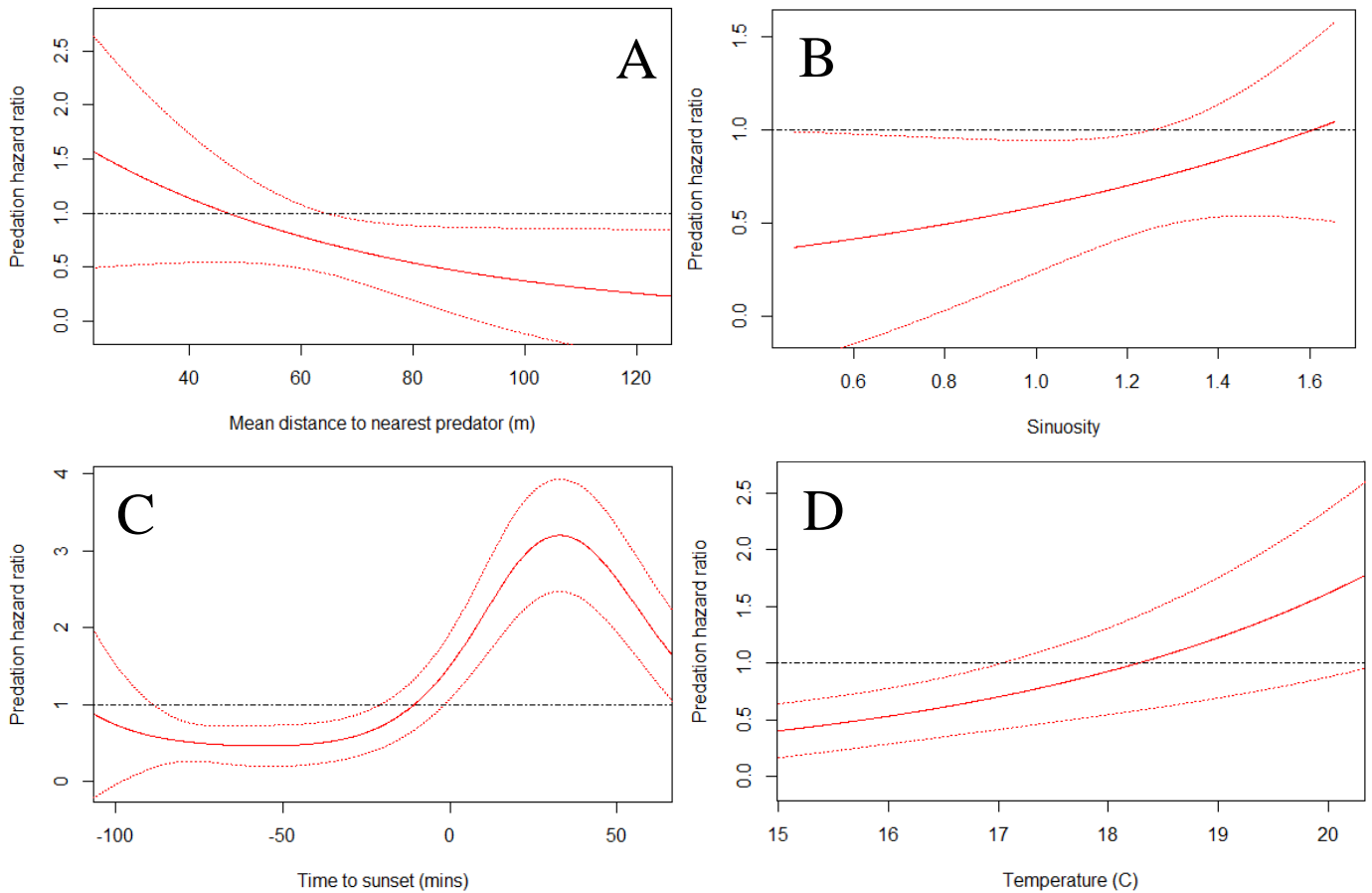
Figure 11: Predicted predation hazard ratio given the range of observed values for (A) mean predator distance (m), (B) sinuosity, (C) time to sunset (minutes), (D) temperature (Celsius) from the most parsimonious Cox Proportional Hazard model. Predictions for each plot are simulated while holding the other variables constant at their median value. Red solid line depicts the estimate, and red dotted lines depict the lower and upper 95% confidence interval. Dashed horizontal black line depicts a predation hazard ratio of 1, i.e., unchanged predation hazard ratio over median conditions.

3.9. South Delta-wide extrapolation of Predation Risk Model

Using the most parsimonious fine-scale spatial-temporal Predation Risk Model, we attempted to predict predation hazard ratio estimates throughout the South Delta at a 1-km resolution. The most parsimonious model included mean predator distance, therefore, we used the most parsimonious Predator Density Model as a submodel to the Predation Risk Model (while incorporating the equation 6 conversion as described in the methods). The Predator Density Model did include the number of SAV patches, which we estimated using side-scan sonar in our study sites. To estimate the number of SAV patches per 1-km site throughout the South Delta, we used a remote-sensed 2015 SAV GIS layer produced by researchers at UC Davis (Hestir et al. 2008, GIS data provided by K. Shapiro, UC Davis).

Because temperature was the only temporally-varying environmental covariate, we predicted what the predation hazard ratio would be throughout the South Delta given different temperature scenarios.

We ran a scenario at the minimum, mean, and maximum temperatures recorded in the lower San Joaquin during the field season, which was scheduled to co-occur with peak juvenile salmon outmigration. Those values were approximately 13º, 16º and 19º Celsius. The per 1-km predation hazard ratios estimated for the 13º scenario were tightly clustered around 0.4, suggesting that a water temperature of 13º will lead to a decreased predation risk throughout the South Delta (relative to median conditions experienced during the Spring of 2017) (Fig. 12). The predation hazard ratios for the 16º scenario ranged from 0.8 to 1.5, suggesting that 16º water can increase or decrease predation risk depending on the site. The predation hazard ratios for the 19º scenario ranged from 1.9 to 3.4, with a much wider spread than the other two temperature scenario distributions. This suggests that at 19º, predation risk is increased over median conditions throughout the South Delta, and can be as high as a threefold increase. Mapping of the predation hazard ratios for the different temperature scenarios reveal that the highest risk areas tend to be in the southern portions of the South Delta, with 1-km segments on the lower San Joaquin River near the Head of Old River having notably high predation risk estimates (Figs. 13 - 15; refer to Supplemental Figs. 5-16 for higher resolution quadrant maps).
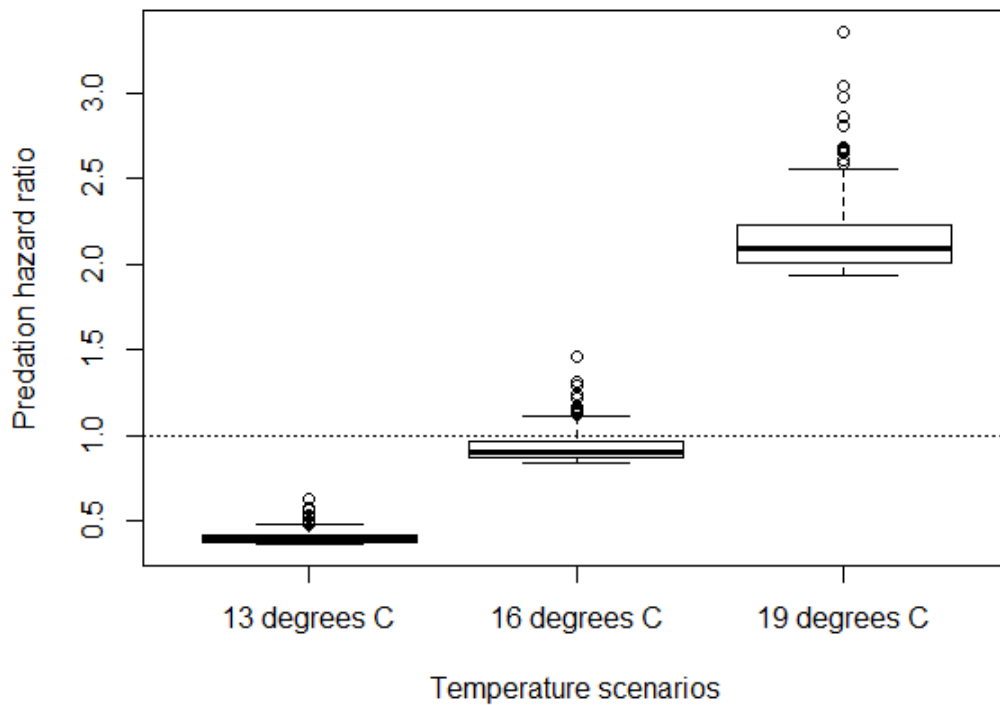
Figure 12: Boxplots of predicted predation hazard ratios per 1-km site (309 in total) per temperature scenario (13º, 16º, and 19º). Dashed horizontal black line depicts a predation hazard ratio of 1, i.e., unchanged predation hazard ratio over median conditions. Bold horizontal lines within boxplot boxes represent median values; lower and upper horizontal lines of the box represent 25th and 75th percentile values; upper and lower horizontal dashes beyond the boxes represent the 75th and 25th percentiles ± 1.5 times the interquartile range (distance from 25th to 75th percentile); values beyond these are considered outliers and are represented with empty circles.
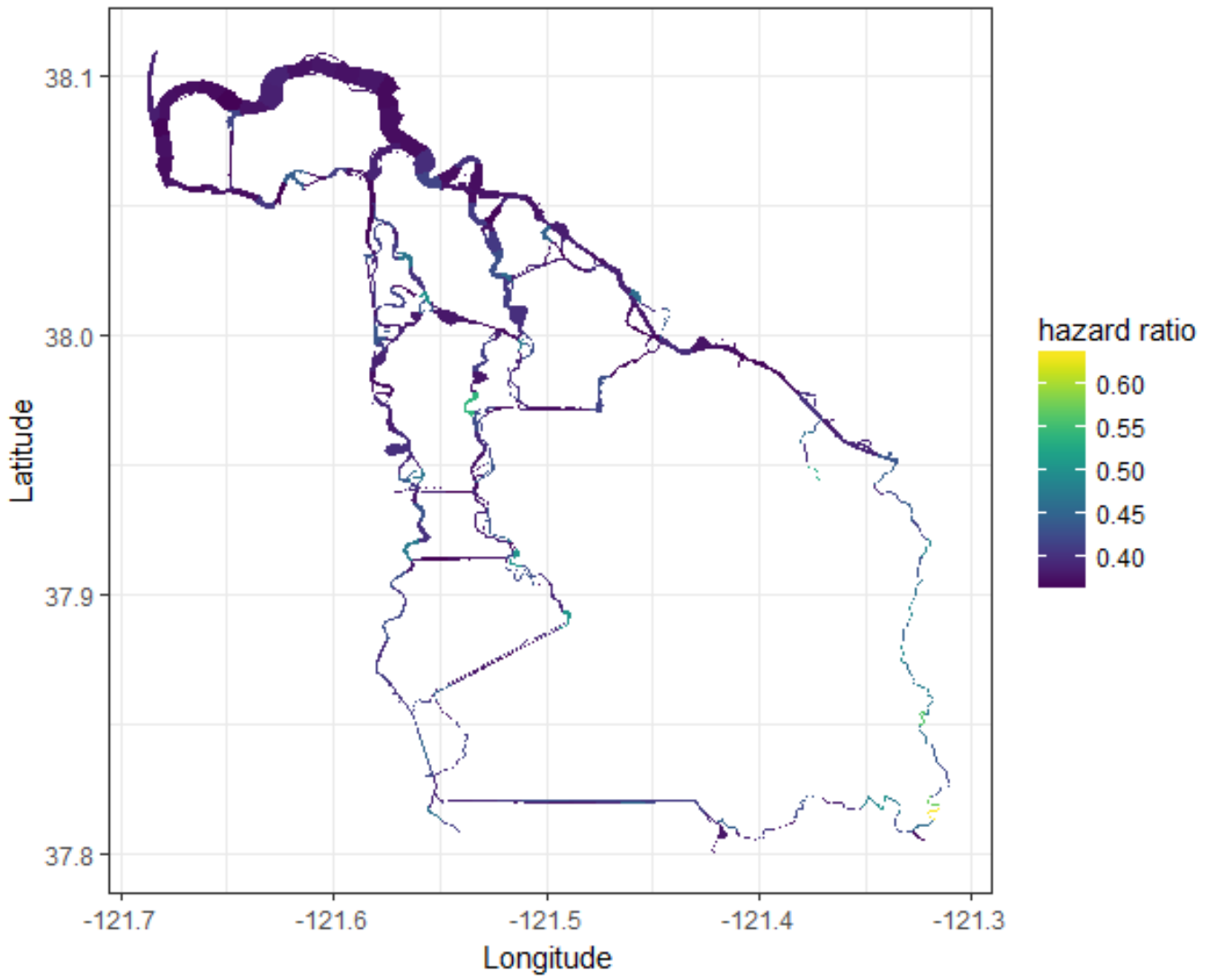
Figure 13: 1-km Predation hazard ratio predictions for the 13º (C) temperature scenario throughout the South Delta
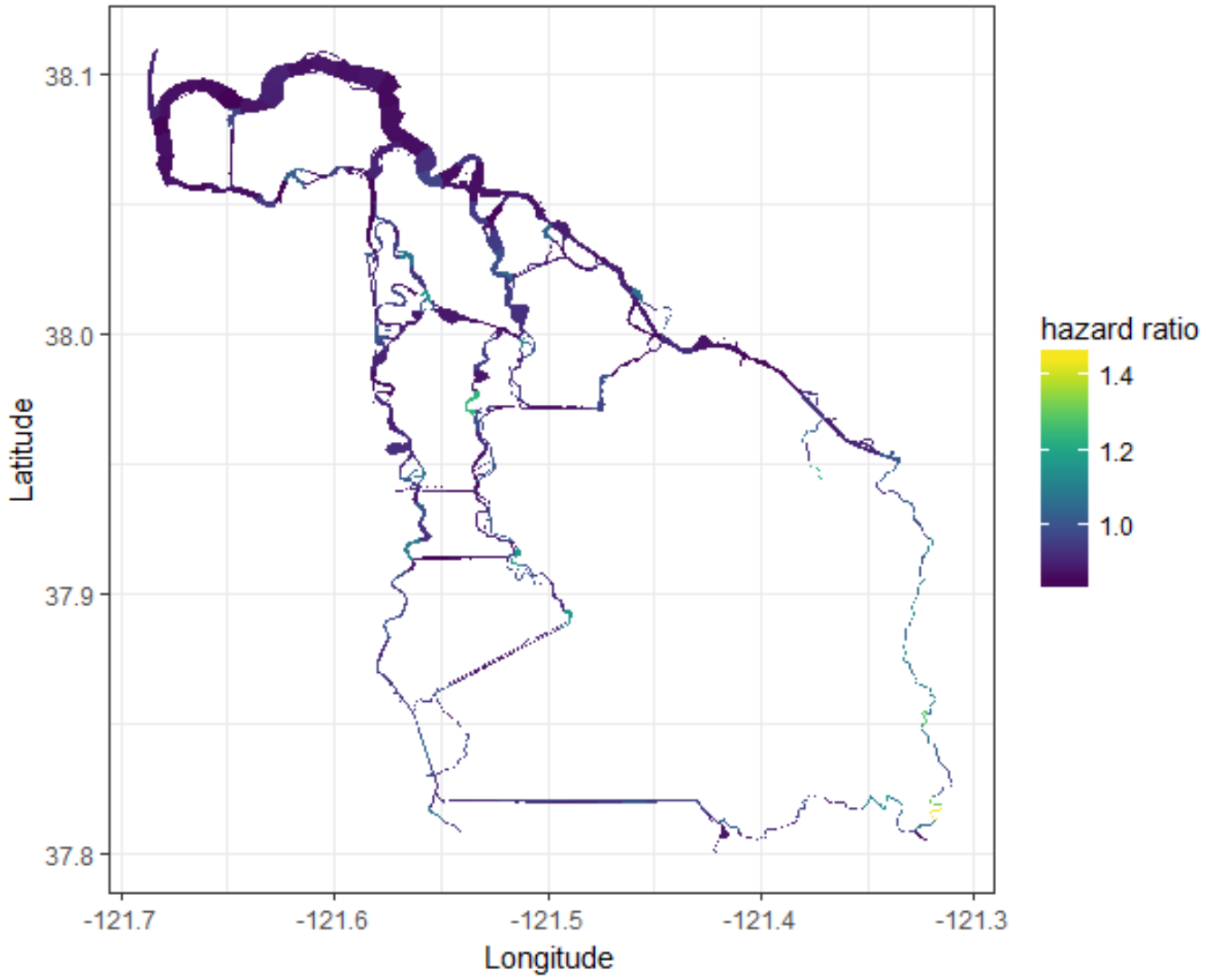
Figure 14: 1-km Predation hazard ratio predictions for the 16º (C) temperature scenario throughout the South Delta
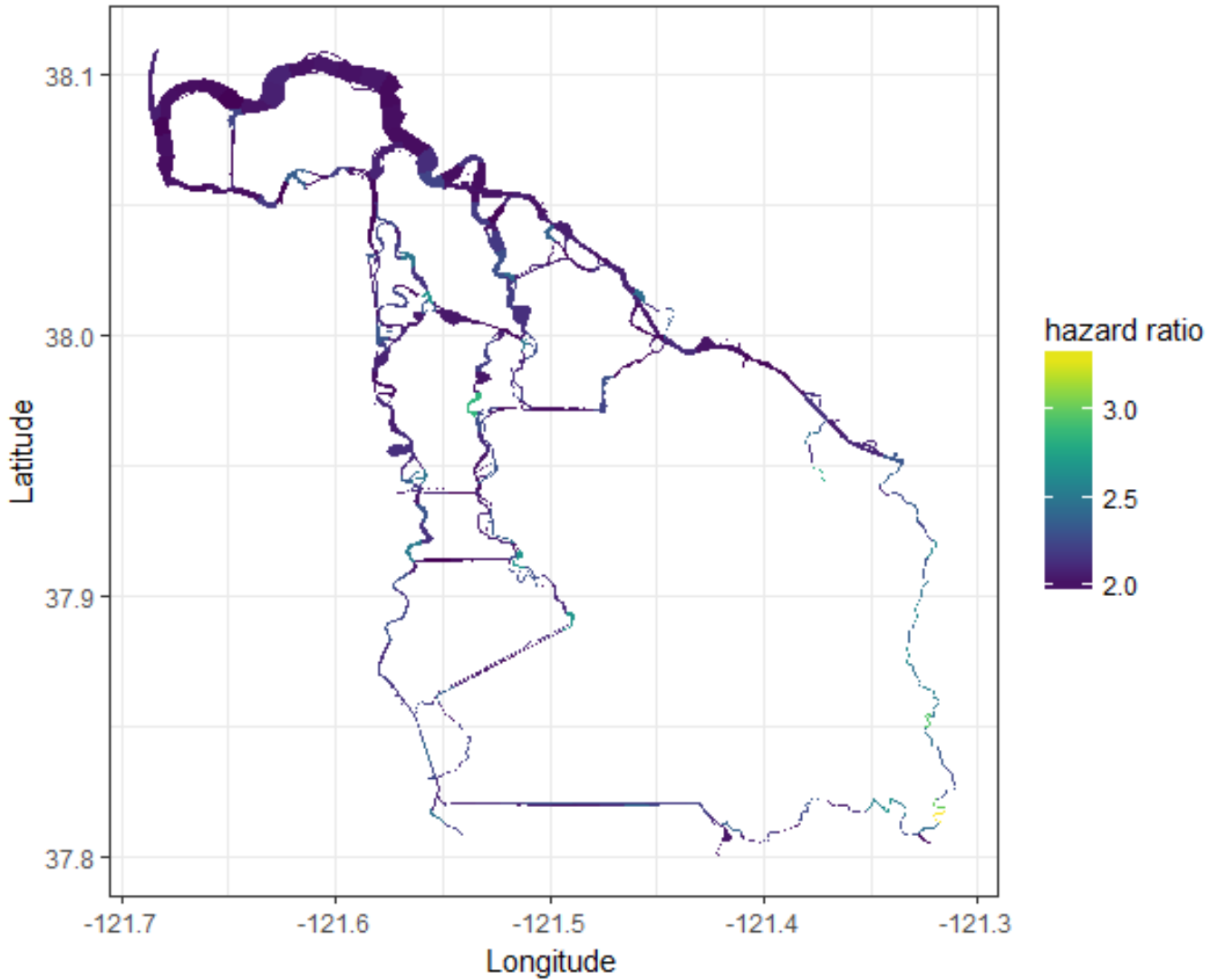
Figure 15: 1-km Predation hazard ratio predictions for the 19º (C) temperature scenario throughout the South Delta

4. Discussion

We developed a statistical model to describe within season temporal changes in predation risk. In addition, we also developed spatially-explicit statistical models describing both predator densities and predation risk. Overall, these models suggest that predation risk for salmonids and other similar prey species in the South Delta in the spring of 2017 were strongly influenced by temperature, time of day, and sinuosity, and to a lesser degree light levels and submerged aquatic vegetation. The direction and form of all discovered relationships between these variables and both predation and predator densities are conguent with the *a priori* expectations, lending some degree of credance to the most parsimonious models.

It is essential to put these relationships elucidated during the 2017 season in a broader context. The 2017 water year was an exceptionally wet year, with vast amounts of water draining into the Delta from both the Sacramento and San Joaquin River drainages. The 2017 water year had the highest annual precipitation index for the Northern Sierras and the second highest index for the San Joaquin River basin from a dataset beginning in 1964 (CDWR 2018). The spring season (during which sampling occurred) was no exception, with many portions of the South Delta closed to recreational boating due to the extremely high water levels. Therefore, the predator and predation relationships discerned in this study may only be representative of conditions during exceptionally wet years. Anecdotal information from fishing guides suggested that striped bass densities were low during the spring 2017 in the Delta, and they believed that striped bass were drawn into the major river systems, upstream of the Delta, in larger numbers than usual due to the large river flows. This would suggest that one of the major predator species was only present in low densities during our study. Furthermore, water velocities in some study sites in the more crossectionally constrained (and leveed) portions of the lower San Joaquin River (from Mossdale to Stockton) were markedly fast, up to 3.5 m/s. At such velocities, it is possible that some predators would be less effective at capturing passing prey (or a baited PER). Comparing the percent of predated PERs at a single site (site 25) between this study and a previous project during the drought years of 2014 and 2015 (Hayes et al. 2017) lends support to such a theory (Fig. 16). Overall, such evidence suggests that any extrapolation from the relationships described in this study should be done with caution unless the goal is to predict predation risk in extremely wet years.
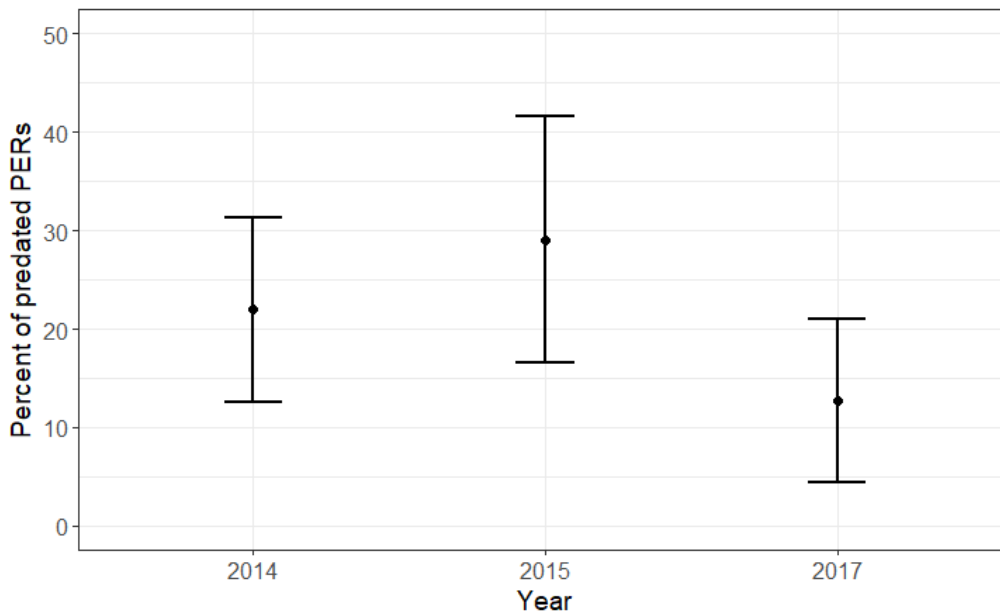

Figure 16: Mean percent of predator PERs at site 25 during a previous project occurring in 2014 and 2015 versus during 2017 (this study). Error bars represent 95% confidence intervals. In all three years, PERs were deployed in the same cross-section of the river.

This study has provided an easily repeatable methodology for quantitatively exploring the role of environmental conditions on predator-prey dynamics in the Delta in many different habitat types and water years. A study such as this one, spanning several years of various water conditions, would likely improve the models developed here.

Some important limiations of this study warrant discussion. Firstly, we attempted to discern the predictors of predation risk by investigating the densities and relative predation rates of predators. However, we did not investigate how environmental covariates may influence juvenile salmonid distribution, health, and overall vulnerability to predation. Future studies should attempt to pair a study similar to this one with studies attempting to discern salmonid distribution and condition. Secondly, PERs only sample the upper one meter of the water column, and also do not effectively sample the littoral margins of the waterway channel, and therefore predation risk estimates as measured by PERs are not representative of the entire cross-section of a waterway.

Management of water and ecological resources in the Delta are contentious issues, and involve multiple resource agencies, stakeholders, and academic institutions. Increasingly, managament actions are being thoroughly evaluated before implementation using physical and ecological models. Many of these models, particularly those concerning the impacts of water and habitat management on imperiled native fish populations, attempt to incorporate the role of changing environmental and habitat variables on the suceptibility of these populations to predation. However, the mechanisms and relationships needed to make these evaluations are largely unknown, and are currently being informed by data from few small-scale case studies. Our study is the first step in providing these models with predation data on the relevant landscape scale, further improving the ability of these models to accurately predict the ecological ramifications of significant management decisions.

5. *Next steps*

Ultimately, our goal is to generate spatially and temporally robust estimates of salmonid predation risks as a way to reveal plausible mechanisms that result in reduction of survivorship. Although juvenile salmonids may only spend weeks to months in the Delta co-occurring with fish predators, substantial predation mortality may occur in high density areas. We will compare our results with existing known predation "hot spots" (Grossman et al. 2013) and identify whether or not there is concordance between the two. This will allow us to generate hypotheses regarding predation mechanisms and also improve model fidelity. Predator control is not likely to be effective without an understanding of the environmental conditions that affect invasive predator success. In combination with habitat data, we will be able to make inferences about conditions under which various fish predators pose the greatest risk.

Furthermore, it is hypothesized that mortality from predation is a significant predictor of survivorship (Grossman et al. 2013, Michel et al. 2015). However, to what degree predation is the cause of salmonid mortality is largely unknown, and it is possible mortality from predation may be small relative to mortality brought about, for example, by water extraction activities, disease, or lethally high water temperatures. High resolution spatially- and temporally-explicit survival estimates exist for many

Central Valley salmonid populations over many years. We will couple overall survivorship from these telemetry studies with predation risk estimates to quantify whether or not and under which circumstances fish predation is a substantial component of total mortality.

Acknowledgements

Hydro-acoustic surveys being performed using two Dual-Identification Sonar (DIDSON) cameras on the small boat "Osprey" (B. Lehman).

6. References

Akaike, H. 1974. A new look at the statistical model identification. IEEE Transactions on Automatic Control 19 (6): 716–723.

Buchanan, R. A., Skalski, J. R., Brandes, P. L., Fuller, A. 2013. Route Use and Survival of Juvenile Chinook Salmon through the San Joaquin River Delta. North American Journal of Fisheries Management 33:216-229.

Burnham K. P., Anderson D. R. 2002. Model selection and multimodel inference: a pratical information-theoretic approach. New York, New York, USA: Springer-Verlag.

Čada, G. F., M. D. Deacon, S. V. Mitz, Bevelhimer, M.S. 1997. Effects of water velocity on the survival of downstream-migrating juvenile salmon and steelhead: A review with emphasis on the Columbia river basin. Reviews in Fisheries Science 5:131-183.

Callihan, J. L., Godwin, C. H., Buckel, J. A. 2014. Effect of demography on spatial distribution: Movement patterns of the Albemarle sound-Roanoke river stock of striped bass (Morone saxatilis) in relation to their recovery. Fishery Bulletin 112: 131–143.

Cronkite, G., Enzenhofer, H. J. 2005. A simple adjustable pole mount for deploying DIDSON and split-beam transducers. Canadian technical report of fisheries and aquatic sciences 925(1488–5379).

California Department of Water Resources (CDWR). 2018. Hydroclimate Report: Water Year 2017. Office of the State Climatologist. Available at: https://water.ca.gov/-/media/DWR-Website/Web-Pages/Programs/All-Programs/Climate-Change-Program/Files/Hydroclimate-Report-2017.pdf

Conrad, L. J., Bibian, A. Weinersmith, J. M., Kelly L., DeCarion, D., Young, M. J., Crain, P., Hestir, E. L., Santos, M. J., Sih, A. 2016. Novel species interactions in a highly modified estuary: associations of Largemouth Bass with Brazilian Waterweed Egeria densa. Transactions of the American Fisheries Society. 145 (2): 249-263

Cox, D. R. 1972. Regression models and life-tables. Journal of the Royal Statistical Society. Series B (Methodological) 34:187-220.

Demetras, N. J., Huff, D. D., Michel, C. J., Smith, J. M., Cutter, G. R., Hayes, S. A., Lindley, S. T. 2016. Development of underwater recorders to quantify predation of juvenile Chinook salmon (*Oncorhynchus tshawytscha*) in a river environment. Fishery Bulletin:179-185.

Feyrer, F., Healey, M. P. 2003. Fish community structure and environmental correlates in the highly altered southern Sacramento-San Joaquin Delta. Environmental Biology of Fishes 66(2):123–132.

Freadman, M. A. 1979. Swimming Energetics of Striped Bass (Morone Saxatilis) and Bluefish (Pomatomus Saltatrix): Gill Ventilation and Swimming Metabolism. The Journal of Experimental Biology 83:217.

Fregoso, T., Wang, R.-F., Ateljevich, E., Jaffe, B. E. 2017. San Francisco Bay-Delta bathymetric/topographic digital elevation model (DEM): US Geological Survey data release https://doi.org/10.5066/F7GH9G27.

Garland, R. D., Tiffan, K. F., Rondorf, D. W., Clark, L. O. 2001. Comparison of subyearling fall Chinook salmon's use of riprap revetments and unaltered habitats in Lake Wallula of the Columbia River. Norther American Journal of Fisheries Management. 22(4): 1283-1289.

Grant, W. D., Madsen, O. S. 1986. The continental-shelf bottom boundary layer. Annual review of fluid mechanics, 18(1), 265-305.

Gregory, R. S., Levings, C. D. 1998. Turbidity reduces predation on migrating juvenile Pacific salmon. Transactions of the American Fisheries Society 127:275-285.

Grossman, G. D., Essington, T., Johnson, B., Miller, J. A., Monsen, N. E., Pearsons, T. N. 2013. Effects of fish predation on Salmonids in the Sacramento River – San Joaquin Delta and associated ecosystems. California Department of Fish and Wildlife.

Hateley, J., Gregory, J. 2006. Evaluation of a multi-beam imaging sonar system (DIDSON) as Fisheries Monitoring Tool: Exploiting the Acoustic Advantage. Technical Report.

Hayes, S. A., Huff, D. D., Demer, D. A., Michel, C. J., Cutter Jr., G. R., Demetras, N. J., Lehman, B., Manugian, S. C., Lindley, S. T., Smith, J. M., Quinn, T. P. 2017. Testing the Effects of Manipulated Predator Densities and Environmental Variables on Juvenile Salmonid Survival in the lower San Joaquin River. Report produced by National Marine Fisheries Service (SWFSC) for the California Department of Water Resources:266.

Helfman, G. S. 1986. Fish Behaviour by Day, Night and Twilight. Pages 366-387 in T. J. Pitcher, editor. The Behaviour of Teleost Fishes. Springer US, Boston, MA.

Hestir, E. L., Schoellhamer, D. H, Greenberg, J., Morgan-Kind, T., Ustin, S. L. 2015. The effect of submerged aquatic vegetation expansion on a declining turbidity trend in the Sacramento-San Joaquin River Delta.

Hightower, J. E., Magowan, K. J., Brown, L. M., Fox, D. A. 2012. Reliability of Fish Size Estimates Obtained From Multibeam Imaging Sonar. Journal of Fish and Wildlife Management 4(1):86–96.

Kaeser, A. J, Litts, T. L. 2010. A novel technique for mapping habitat in navigable streams using low-cost side scan sonar. Fisheries. 35(4) 163-174.

Kaeser, A. J., Litts, T. L., Tracy, W. T. 2013. Using low-cost side-scan sonar for benthic mapping throughout the lower Flint River, Georgia, USA. River Research and Applications 29:634-644.

Kjelson, M. A., Brandes, P. L. 1989. The use of smolt survival estimates to quantify the effects of habitat changes on salmonid stocks in the Sacramento-San Joaquin River, California. Pages 100-

115 in C. D. Levings, L. B. Holtby, and M. A. Henderson, editors. Proceedings of the National Workshop on the effects of habitat alteration on salmonid stocks. Canadian Special Publication of Fisheries and Aquatic Sciences.

Lyons, A. J., Turner, W. C., Getz, W. M. 2013. Home range plus: a space-time characterization of movement over real landscapes. Movement Ecology 1:2.

Michel, C. J., Ammann, A. J., Lindley, S. T., Sandstrom, P. T., Chapman, E. D., Thomas, M. J., Singer, G. P., Klimley, A. P., MacFarlane, R. B. 2015. Chinook salmon outmigration survival in wet and dry years in California's Sacramento River. Canadian Journal of Fisheries and Aquatic Sciences 72:1749-1759.

Michel, C. J., Smith, J. M., Demetras, N. J., Huff, D. D, Hayes, S. A. 2018. Non-native Fish Predator Density and Molecular-based Diet Estimates suggest differing impacts of Predator Species on Juvenile Salmon in the San Joaquin River, California. San Francisco Estuary and Watershed Sciences.

Moyle, P. B. 2002. Inland fishes of California. University of California Press.

Nobriga, M. L., Feyrer, F., Baxter, R. D., Chotkowski, M. 2005. Patterns in species composition, life history strategies, and biomass. Estuaries 28 (5) 776-785.

Nobriga, M., Feyrer, F. 2007. Shallow-water piscivore-prey dynamics in the Sacramento-San Joaquin Delta. San Francisco Estuary and Watershed Science Vol.5, Issue 2, Article 4.

Perry, R. W., Skalski, J. R., Brandes, P. L., Sandstrom, P. T., Klimley, A. P., Ammann, A., MacFarlane, B. 2010. Estimating Survival and Migration Route Probabilities of Juvenile Chinook Salmon in the Sacramento-San Joaquin River Delta. North American Journal of Fisheries Management 30:142-156.

Roni, P., Pess, G.R., Beechie, T.J., Hanson, K.M. 2014. Fish-habitat relationships and the effectiveness of habitat restoration. U.S. Dept. Commer., NOAA Tech. Memo. NMFS-645 NWFSC-127.

Savino, J. F., Stein, R. A. 1989. Behavior of fish predators and their prey: habitat choice between open water and dense vegetation. Environmental Biology of Fishes. 24 (4) 287-293.

Stevens Jr., D. L., Olsen, A. R. 2004. Spatially Balanced Sampling of Natural Resources. Journal of the American Statistical Association. 99:465, 262-278.

Sweka, J. A., Hartman, K. J. 2003. Reduction of Reactive Distance and Foraging Success in Smallmouth Bass, Micropterus dolomieu, Exposed to Elevated Turbidity Levels. Environmental Biology of Fishes 67:341-347.

Therneau, T. M., Grambsch, P. M. 2000. The Cox Model. Pages 39-77 Modeling Survival Data: Extending the Cox Model. Springer New York, New York, NY.

Tušer, M., Frouzová, J., Balk, H., Muška, M., Mrkvička, T., Kubečka, J. 2014. Evaluation of potential bias in observing fish with a DIDSON acoustic camera. Fisheries Research 155(Supplement C):114–121.

Zucchini, W., Borchers, D. L., Erdelmeier, M., Rexstad, E., Bishop, J. 2007. WiSP 1.2.4. Institut fur Statistik und Okonometrie, Geror-August-Universitat Gottingen, Platz der Gottinger Seiben 5, Gottingen, Germany.

7. *Appendix*

Supplemental Table 1. Summary statistics from each sampling day of the 2017 field season (refer to Figure 4 for location of each sample site). Repeat site numbers are in bold

Dates	Site	Predated PERs	Total Deployed	Percent Predated PERs	Week	Region
4/3/2017	**28**	6	64	9.4	1	Mildred Island, Turner Cut, Columbia Cut
4/4/2017	**1**	8	49	16.3	1	Lower San Joaquin River
4/5/2017	**25**	6	31	19.4	1	Upper San Joaquin River
4/6/2017	3	2	52	3.8	1	Lower Old River
4/7/2017	6	5	71	7.0	1	Mildred Island, Turner Cut, Columbia Cut
4/8/2017	8	9	45	20.0	1	Lower Old River
4/10/2017	**1**	4	47	8.5	2	Lower San Joaquin River
4/11/2017	**25**	6	38	15.8	2	Upper San Joaquin River
4/12/2017	**28**	5	41	12.2	2	Mildred Island, Turner Cut, Columbia Cut
4/13/2017	10	0	23	0.0	2	Lower Old River
4/14/2017	11	5	51	9.8	2	Mildred Island, Turner Cut, Columbia Cut
4/15/2017	12	10	45	22.2	2	Lower San Joaquin River
4/17/2017	**25**	2	47	4.3	3	Upper San Joaquin River
4/18/2017	**28**	5	54	9.3	3	Mildred Island, Turner Cut, Columbia Cut
4/19/2017	**1**	6	41	14.6	3	Lower San Joaquin River
4/20/2017	13	1	74	1.4	3	Upper San Joaquin River
4/21/2017	14	2	69	2.9	3	Upper Old River
4/22/2017	16	6	42	14.3	3	Mid San Joaquin River
4/25/2017	**28**	2	48	4.2	4	Mildred Island, Turner Cut, Columbia Cut
4/26/2017	**1**	10	53	18.9	4	Lower San Joaquin River
4/27/2017	**25**	6	42	14.3	4	Upper San Joaquin River
4/28/2017	19	7	69	10.1	4	Lower Old River
4/29/2017	22	10	47	21.3	4	Lower Old River
5/1/2017	**1**	5	38	13.2	5	Lower San Joaquin River
5/2/2017	**25**	13	50	26.0	5	Upper San Joaquin River
5/3/2017	**28**	15	45	33.3	5	Mildred Island, Turner Cut, Columbia Cut

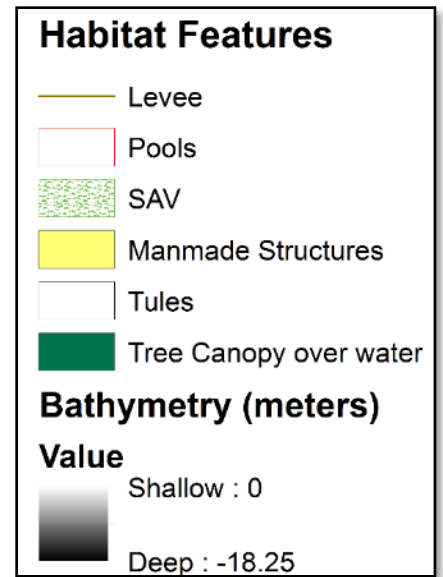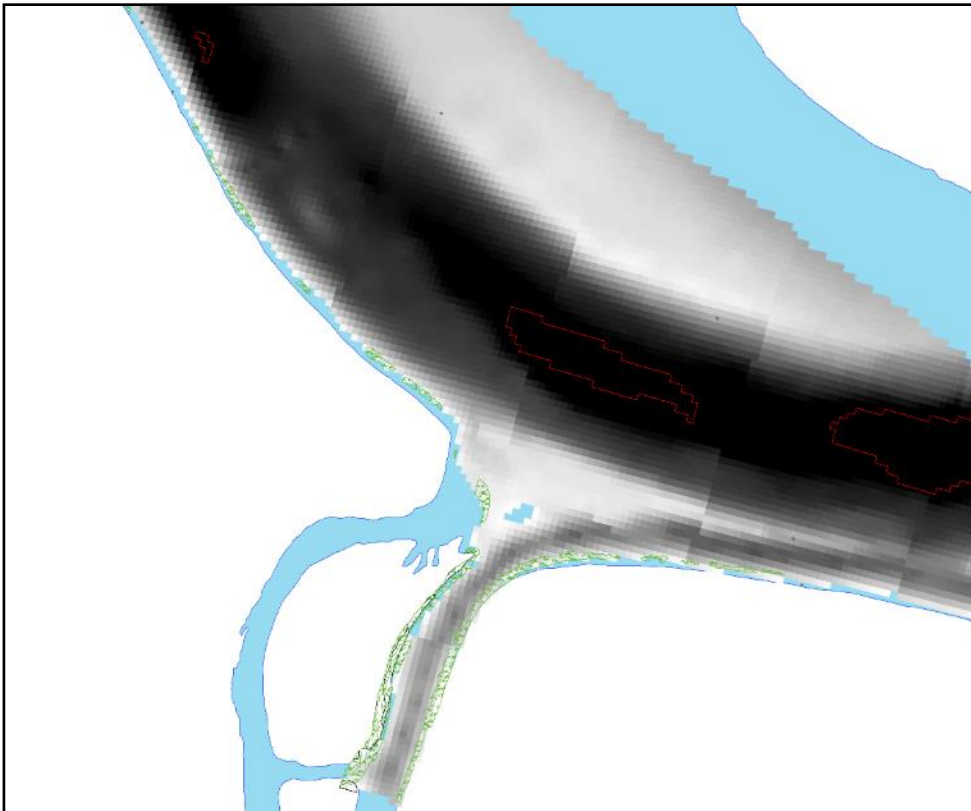| Date						Region
5/4/2017	23	9	41	22.0	5	Upper San Joaquin River
5/5/2017	24	8	45	17.8	5	Lower San Joaquin River
5/6/2017	27	15	58	25.9	5	Mildred Island, Turner Cut, Columbia Cut
5/8/2017	**25**	17	46	37.0	6	Upper San Joaquin River
5/9/2017	**28**	13	36	36.1	6	Mildred Island, Turner Cut, Columbia Cut
5/10/2017	**1**	12	36	33.3	6	Lower San Joaquin River
5/11/2017	33	9	49	18.4	6	Lower San Joaquin River
5/12/2017	34	11	31	35.5	6	Upper Old River
5/13/2017	37	12	52	23.1	6	Franks Tract
TOTAL						
35 days	**20 sites**	**262 predated PERs**	**1670 PERs deployed**	**15.7 % predated PERs**	**6 weeks**	**7 Regions**

Supplemental Table 2. Predator abundance and densities from each sampling day of the 2017 field season (refer to Figure 4 for location of each sample site).

Date	Site	Number of Density Estimates	Mean Total Reach Density (per 10m²)	Standard Error
4/3/2017	28	4	0.2866	0.0162
4/4/2017	1	12	0.1937	0.00377
4/5/2017	25	6	0.2256	0.00713
4/6/2017	3	12	0.2605	0.00383
4/7/2017	6	28	0.1794	0.0032
4/8/2017	8	12	0.2413	0.00201
4/10/2017	1	20	0.2698	0.00297
4/11/2017	25	4	0.1941	0.0121
4/12/2017	28	3	0.1186	0.0125
4/13/2017	10	4	0.1563	0.007
4/14/2017	11	63	0.1455	0.000627
4/15/2017	12	24	0.2209	0.00338
4/17/2017	25	9	0.1042	0.00138
4/18/2017	28	20	0.1738	0.0028
4/19/2017	1	20	0.2548	0.00471
4/20/2017	13	6	0.1197	0.00613
4/21/2017	14	9	0.5061	0.00606
4/22/2017	16	17	0.1464	0.00287
4/25/2017	28	20	0.1011	0.0014
4/26/2017	1	4	0.1205	0.00908
4/27/2017	25	9	0.1253	0.00533
4/28/2017	19	12	0.0734	0.00274
4/29/2017	22	4	0.1176	0.0128
5/1/2017	1	10	0.1415	0.016
5/2/2017	25	6	0.3093	0.0196
5/3/2017	28	12	0.217	0.00416
5/4/2017	23	7	0.1219	0.00496
5/5/2017	24	28	0.0921	0.00123
5/6/2017	27	28	0.0888	0.000961
5/8/2017	25	6	0.5698	0.0148
5/9/2017	28	20	0.1334	0.00182
5/10/2017	1	4	0.1561	0.00668
5/11/2017	33	29	0.0971	0.000936
5/12/2017	34	20	0.2667	0.00119
5/13/2017	37	20	0.105	0.00276
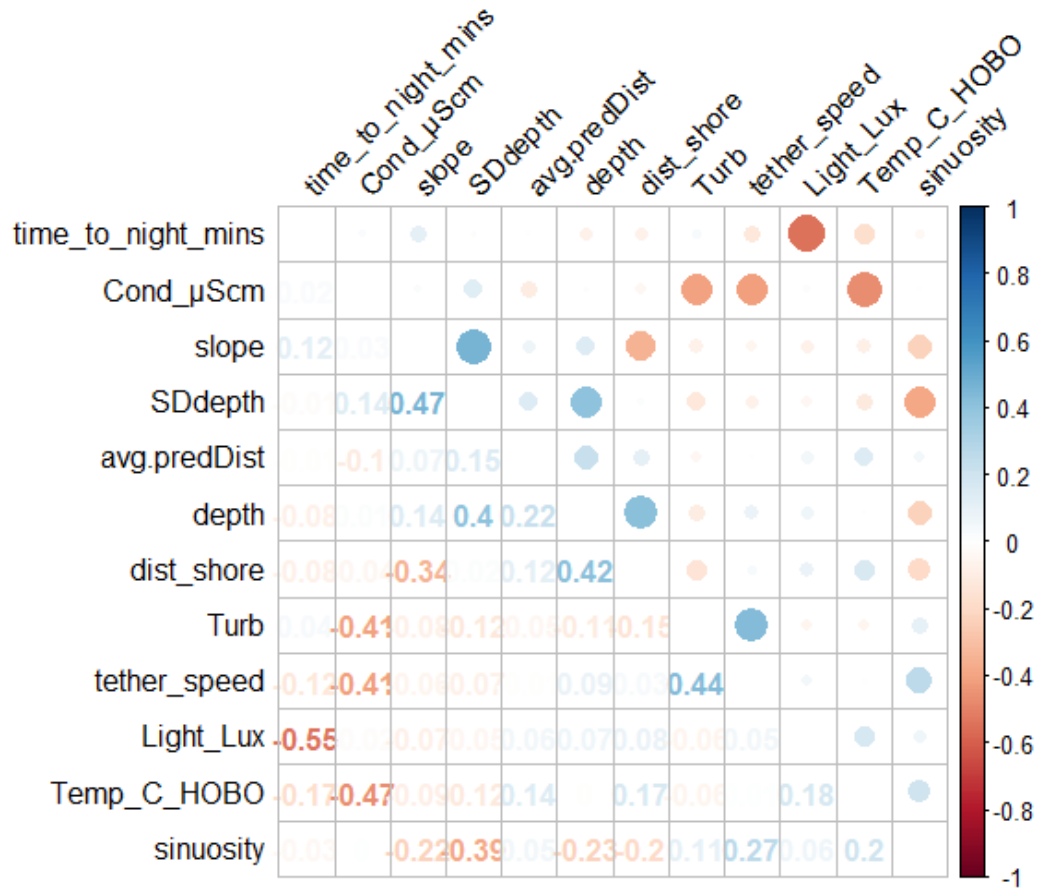
Supplemental Figure 1: Correlation plot for variables used in the Fine-scale spatial-temporal Predation Risk Model. Values represent correlation coefficients. The width of colored dots represents the strength of the correlation, and the color represents the direction of the relationship (positive relationships in blue, and negative relationships in red).
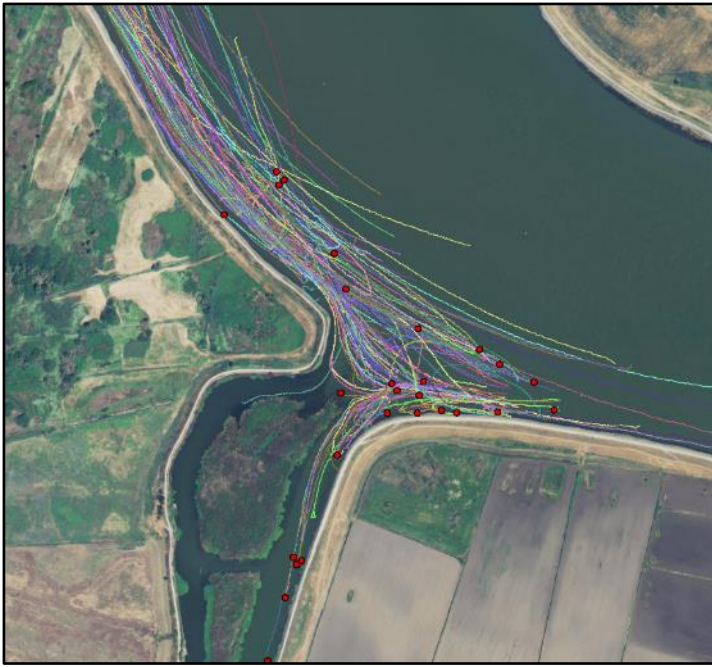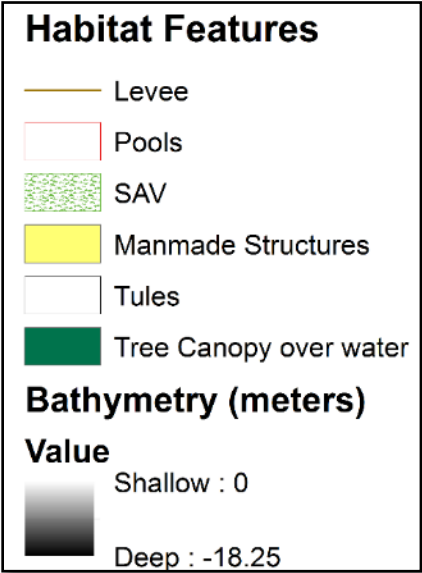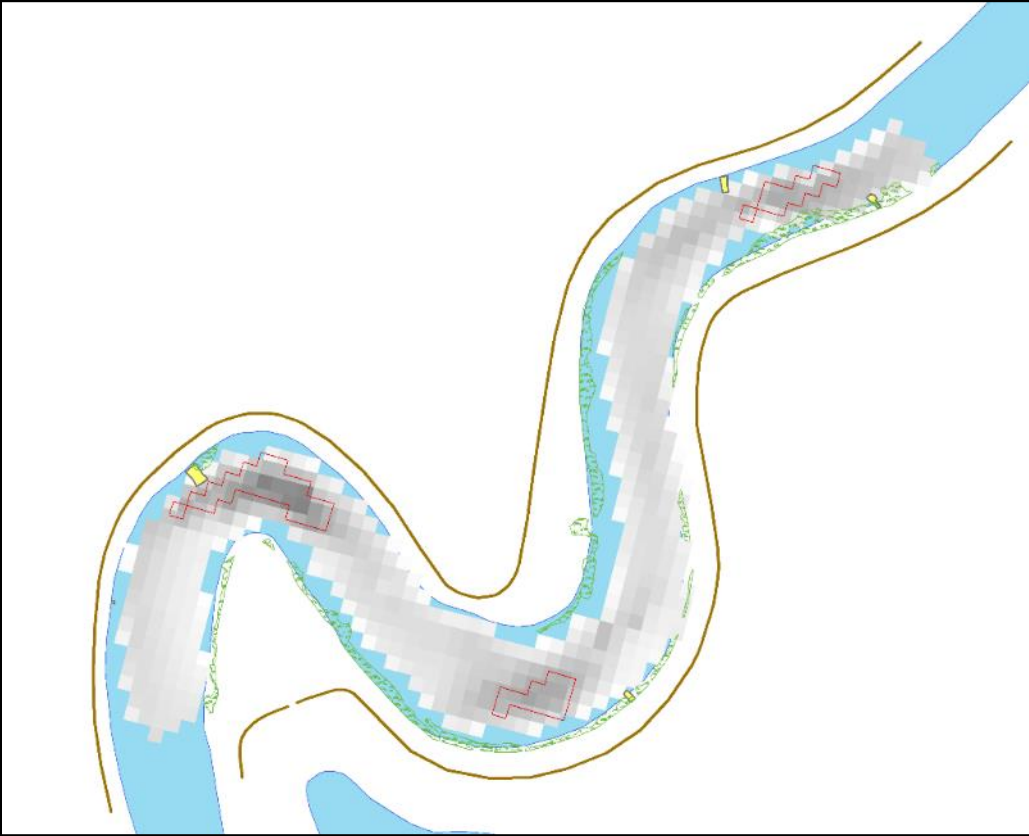
Site 1: San Joaquin River near and including Fisherman's Cut, 1:6000 scale

Habitat Features

— Levee
□ Pools
▤ SAV
▤ Manmade Structures
□ Tules
■ Tree Canopy over water

**Bathymetry (meters)**

Value

Shallow : 0

Deep : -18.25

Supplemental Figure 2: Maps depicting resolution and distribution of different datasets for site 1. Top-left map depicts the tracks of PERs (color coded lines for each unique PER track), and predation events in red dots. Top-right map depicts predators located using DIDSON cameras. Bottom map and associated legend depict the various habitat features collected.

Site 25: San Joaquin River near Haven Acres Marina, 1:3000 scale

Habitat Features

——	Levee
▭	Pools
▦	SAV
▮	Manmade Structures
▭	Tules
▮	Tree Canopy over water

Bathymetry (meters)

Value

Shallow : 0

Deep : -18.25

Supplemental Figure 3: Maps depicting resolution and distribution of different datasets for site 25. Top-left map depicts the tracks of PERs (color coded lines for each unique PER track), and predation events in red dots. Top-right map depicts predators located using DIDSON cameras. Bottom map and associated legend depict the various habitat features collected.

Site 28: Turner Cut near confluence with San Joaquin River, 1:5000 scale
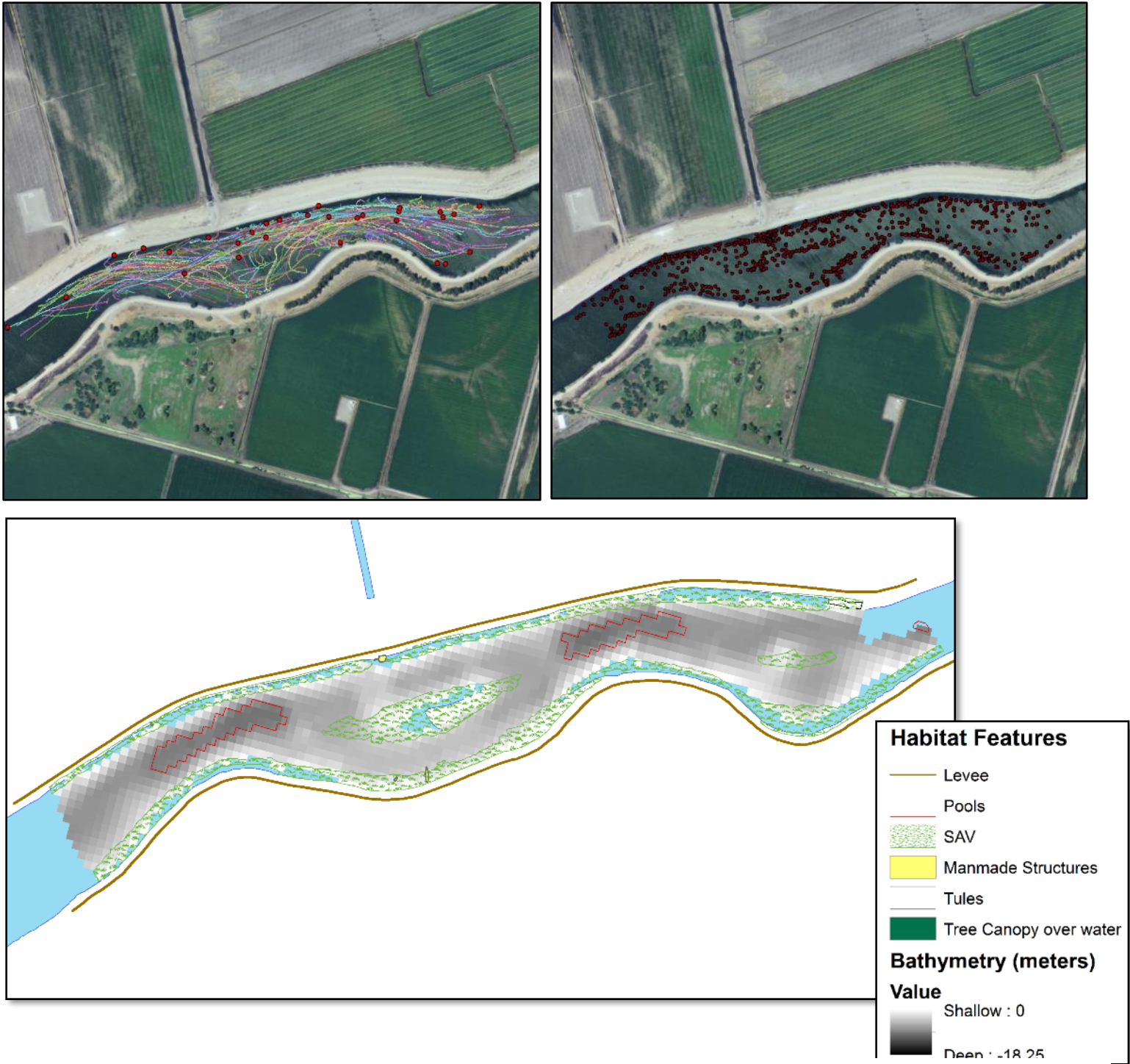
Supplemental Figure 4: Maps depicting resolution and distribution of different datasets for site 28. Top-left map depicts the tracks of PERs (color coded lines for each unique PER track), and predation events in red dots. Top-right map depicts predators located using DIDSON cameras. Bottom map and associated legend depict the various habitat features collected.
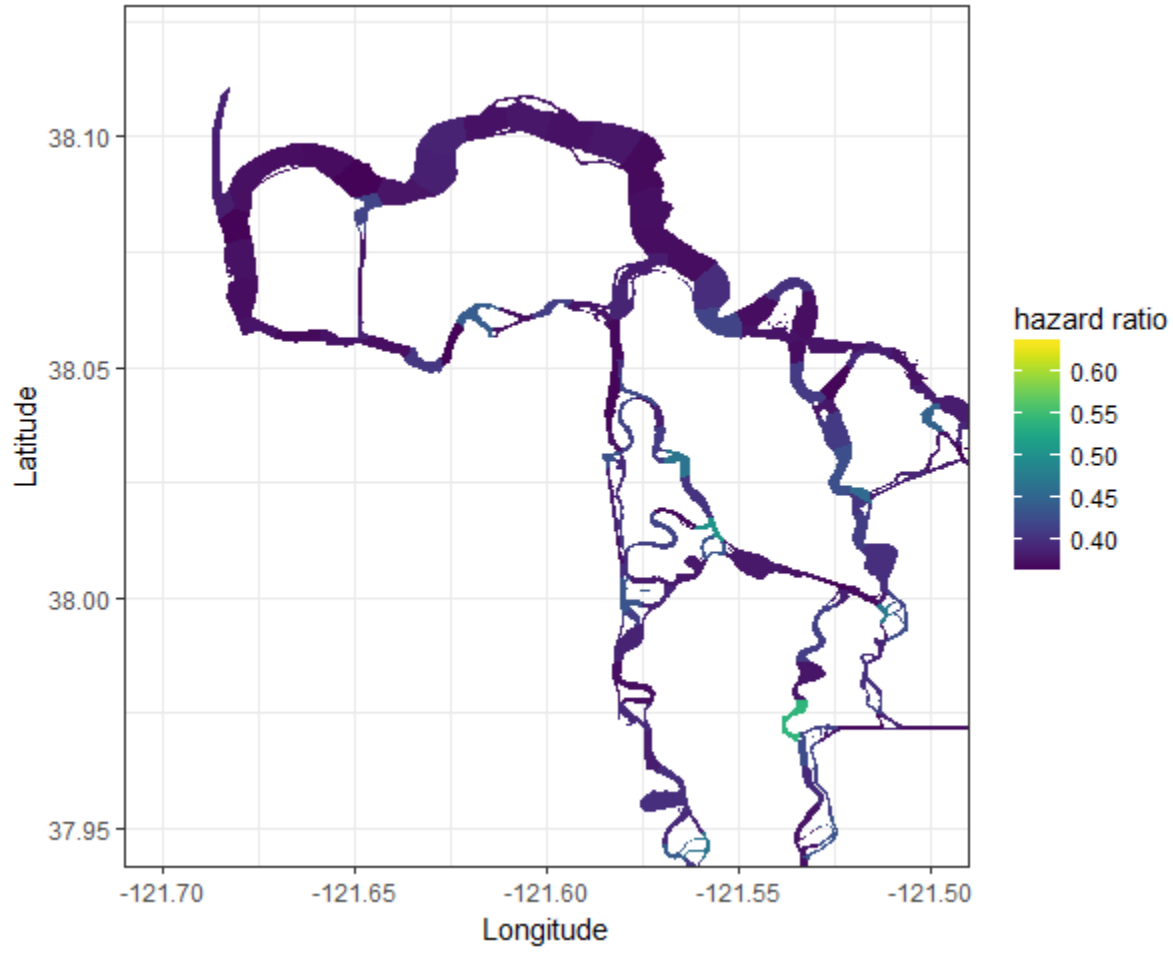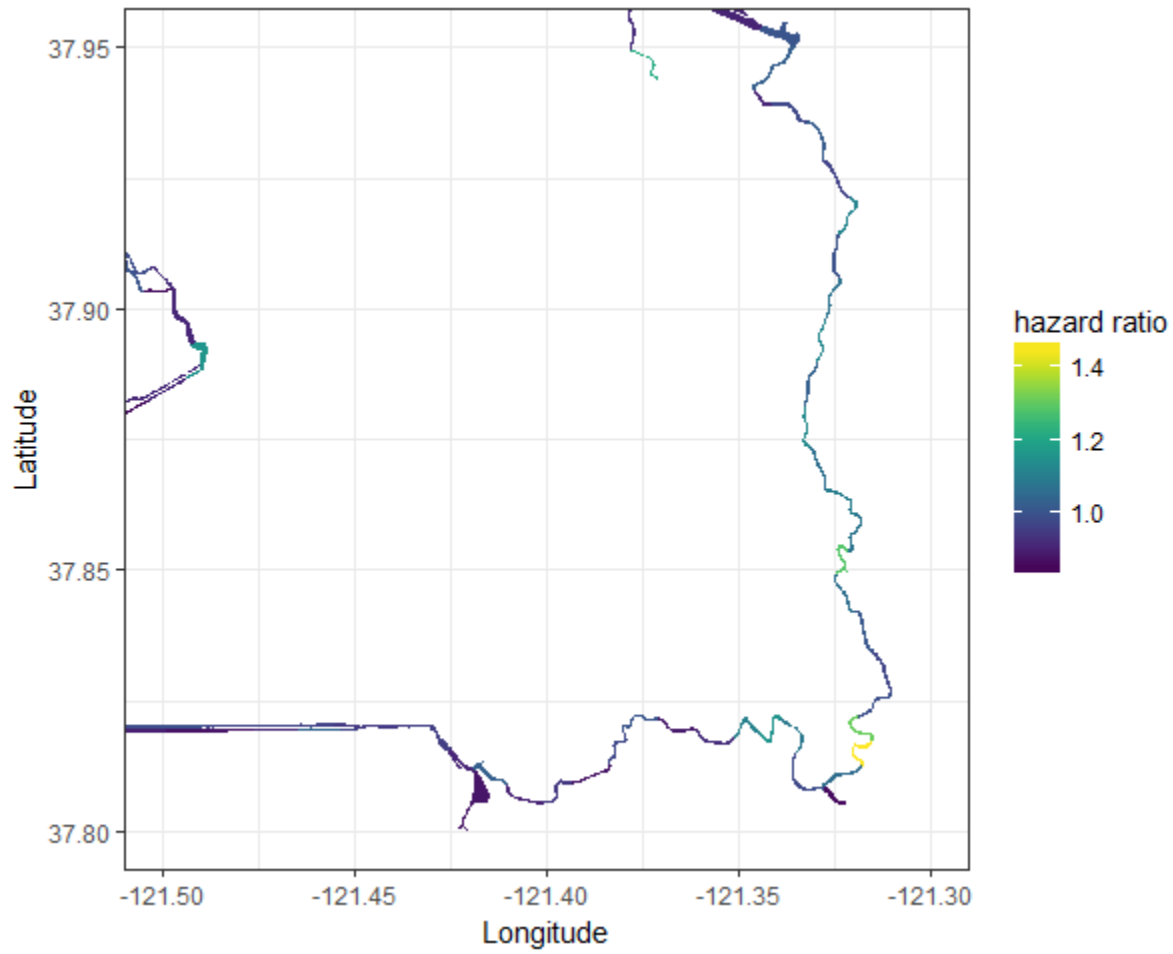
Supplemental Figure 5: 1-km Predation hazard ratio predictions for the 13º (C) temperature scenario, NW quadrant of the South Delta
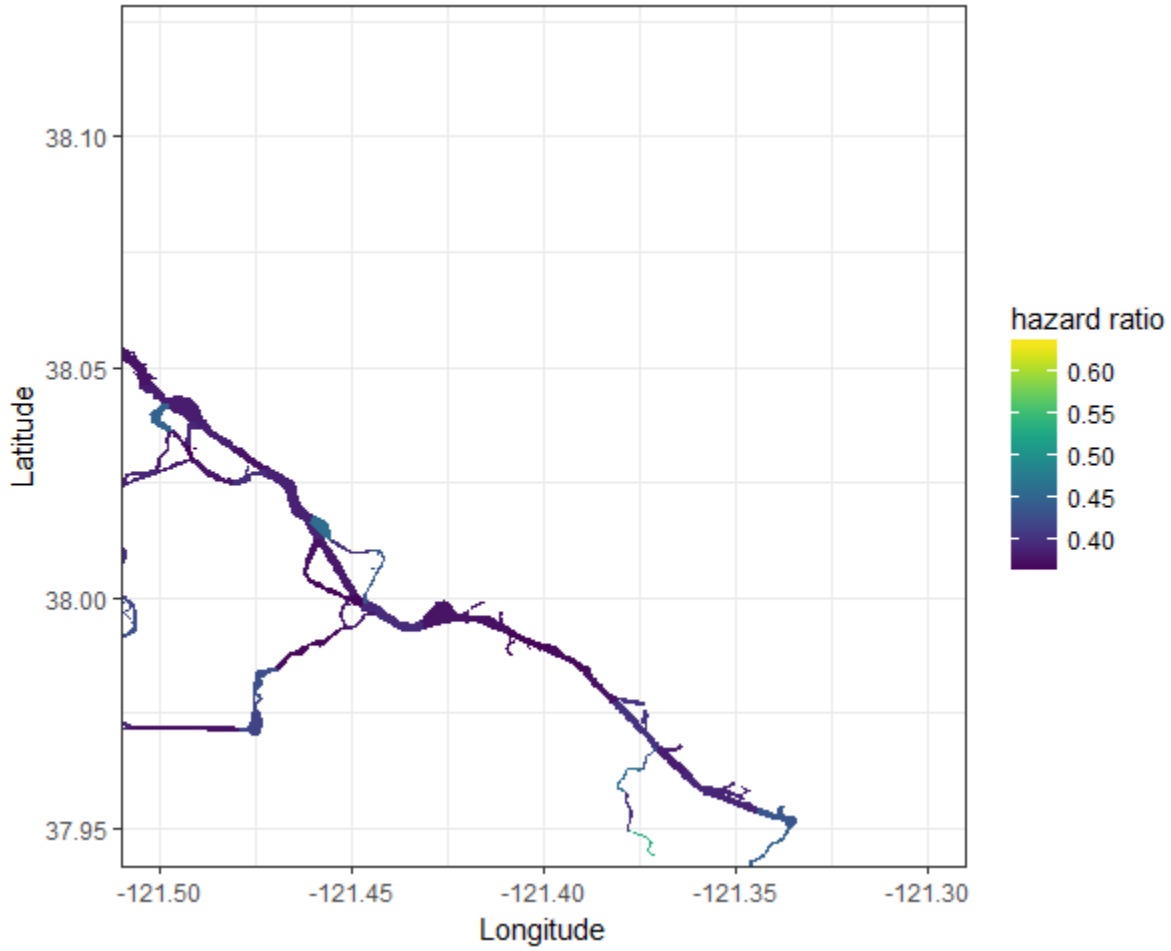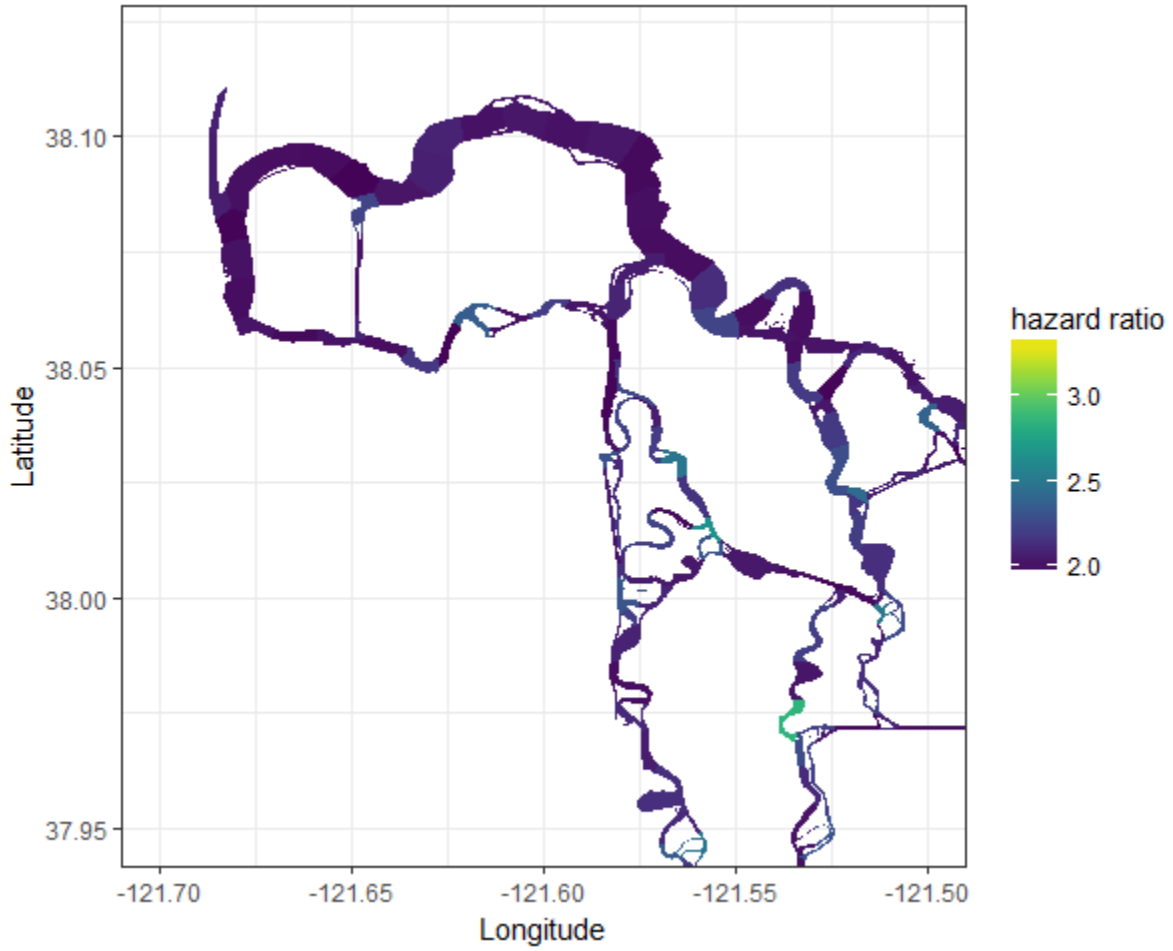
Supplemental Figure 6: 1-km Predation hazard ratio predictions for the 13º (C) temperature scenario, NE quadrant of the South Delta
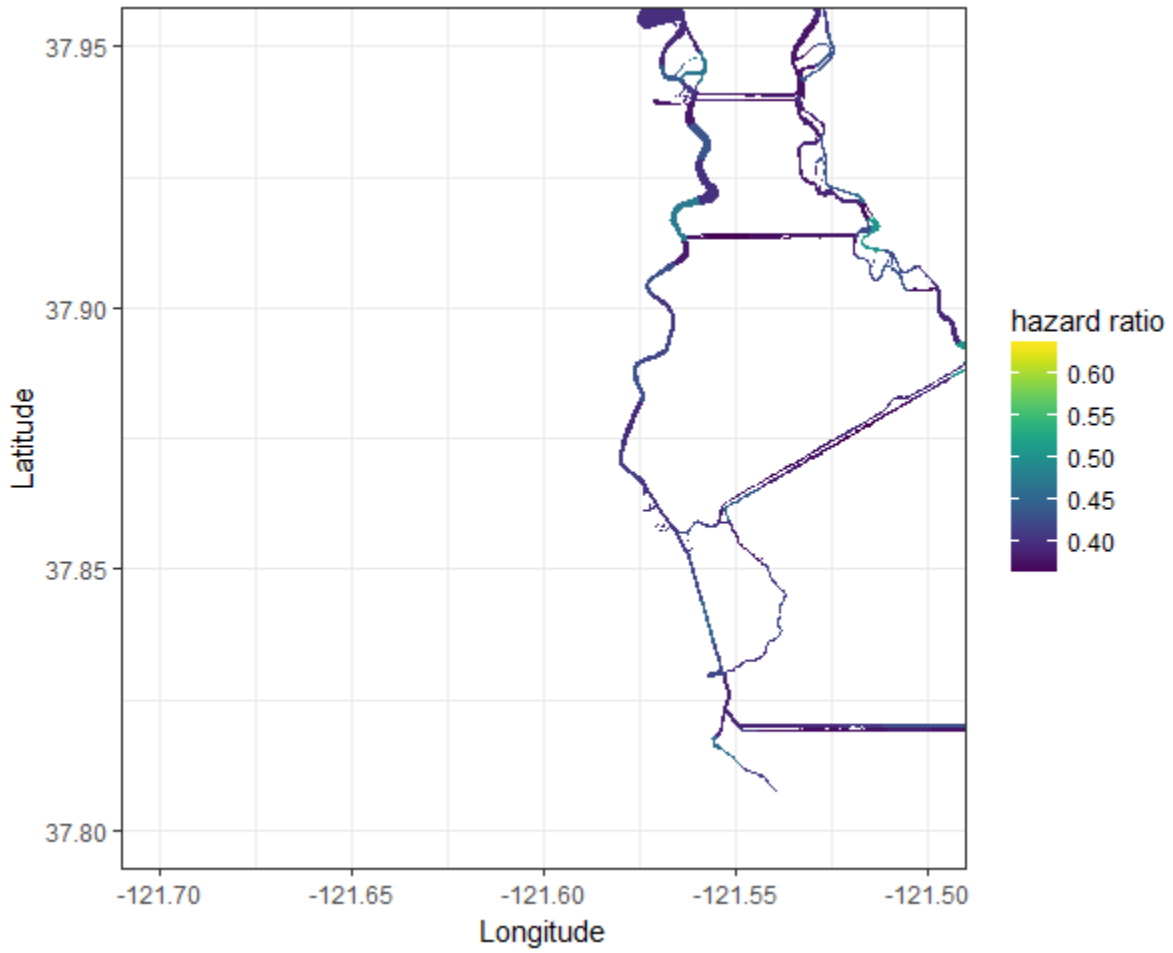
Supplemental Figure 7: 1-km Predation hazard ratio predictions for the 13º (C) temperature scenario, SW quadrant of the South Delta
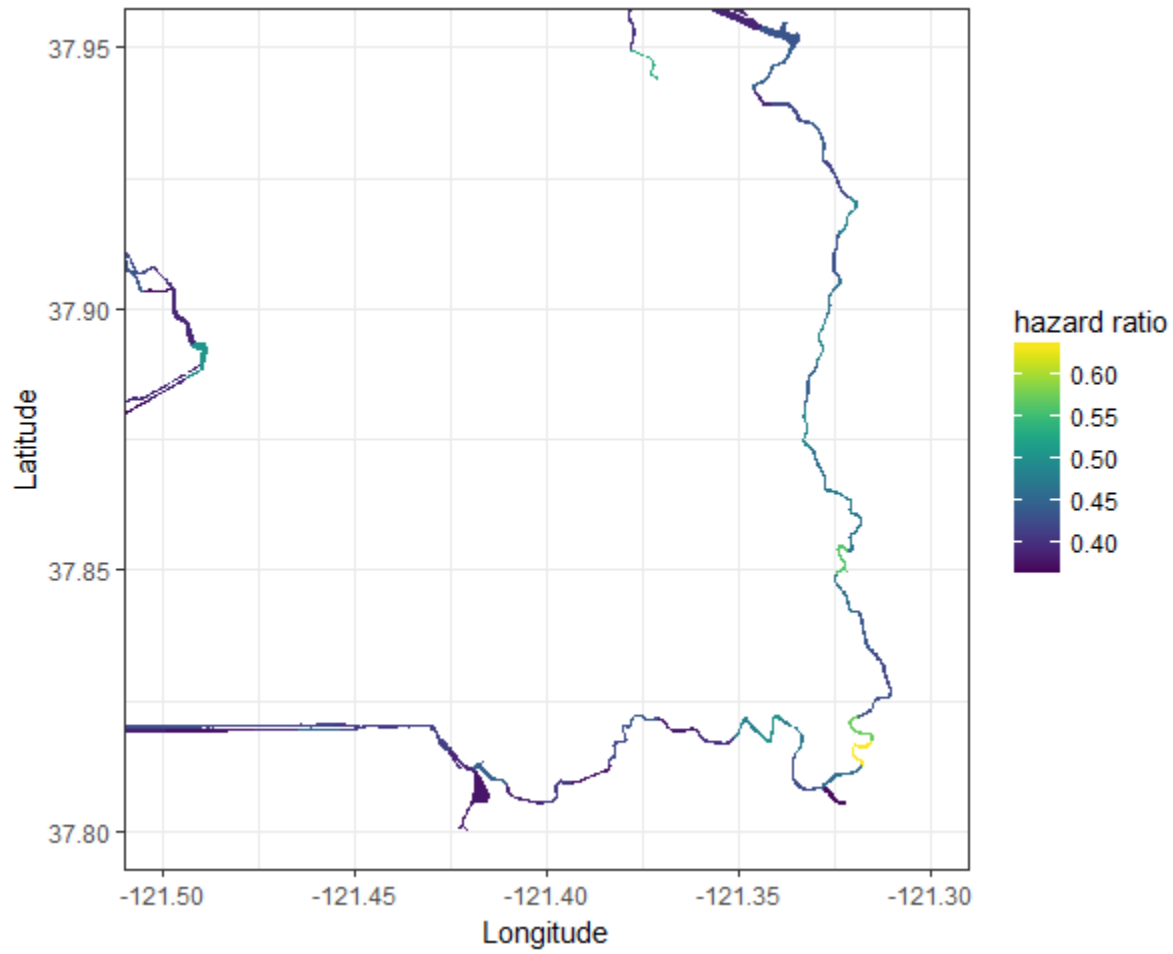
Supplemental Figure 8: 1-km Predation hazard ratio predictions for the 13º (C) temperature scenario, SE quadrant of the South Delta
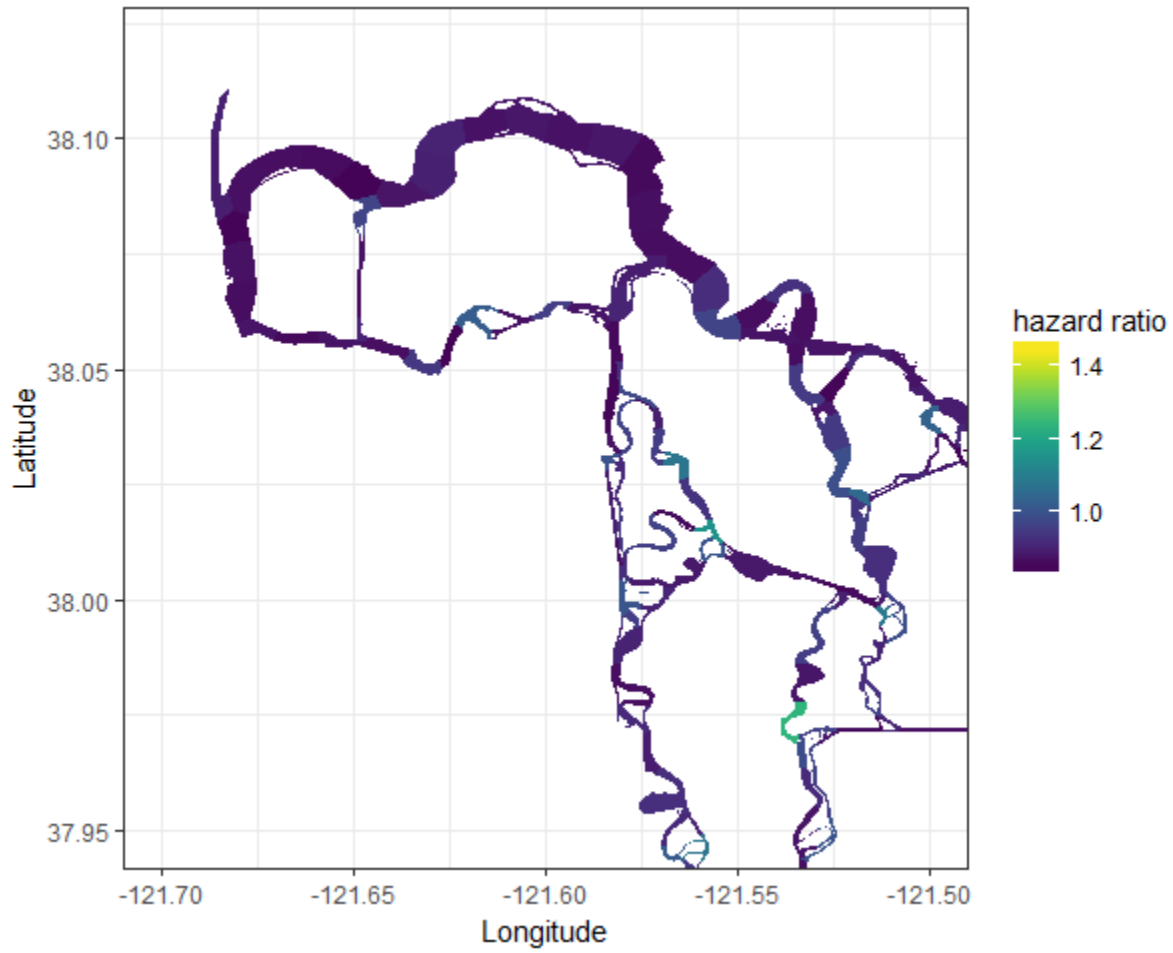
Supplemental Figure 9: 1-km Predation hazard ratio predictions for the 16º (C) temperature scenario, NW quadrant of the South Delta
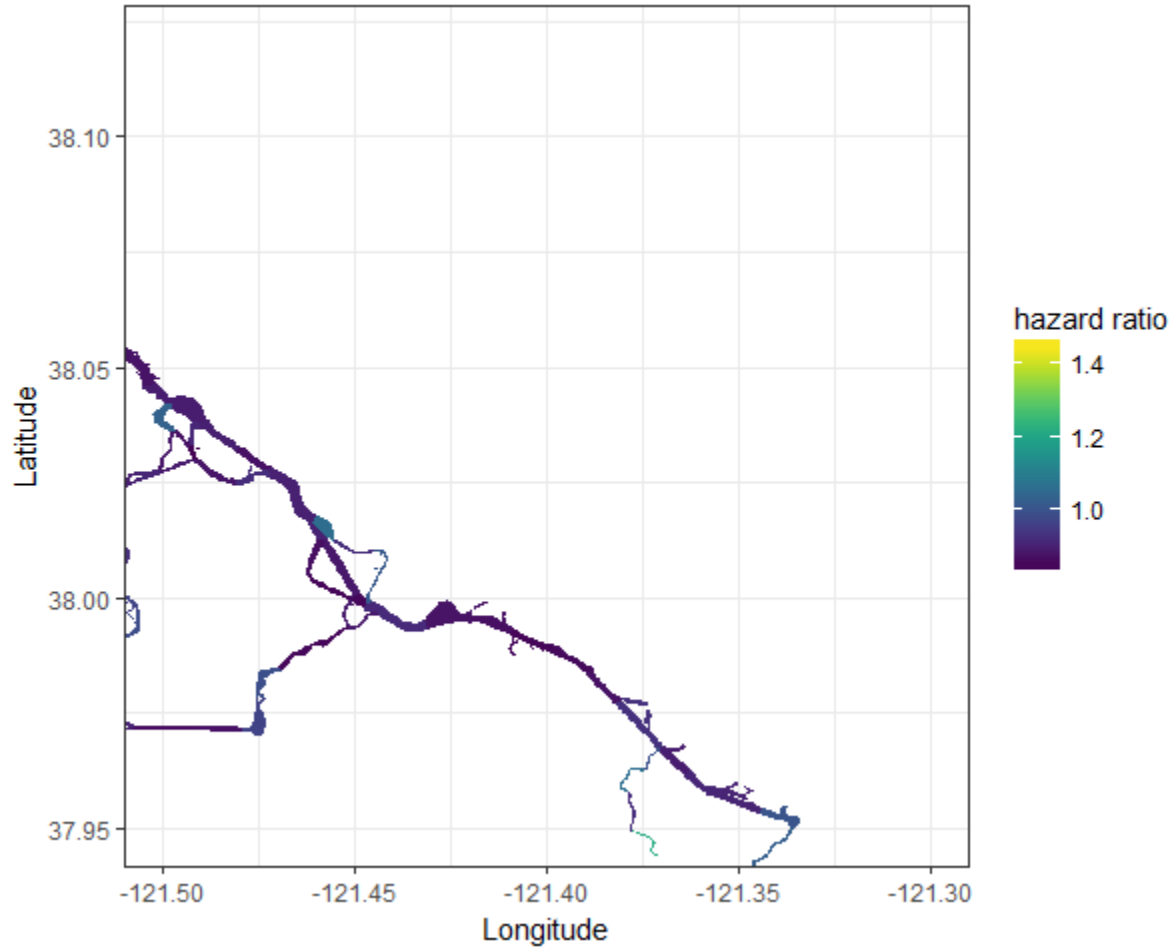
Supplemental Figure 10: 1-km Predation hazard ratio predictions for the 16º (C) temperature scenario, NE quadrant of the South Delta
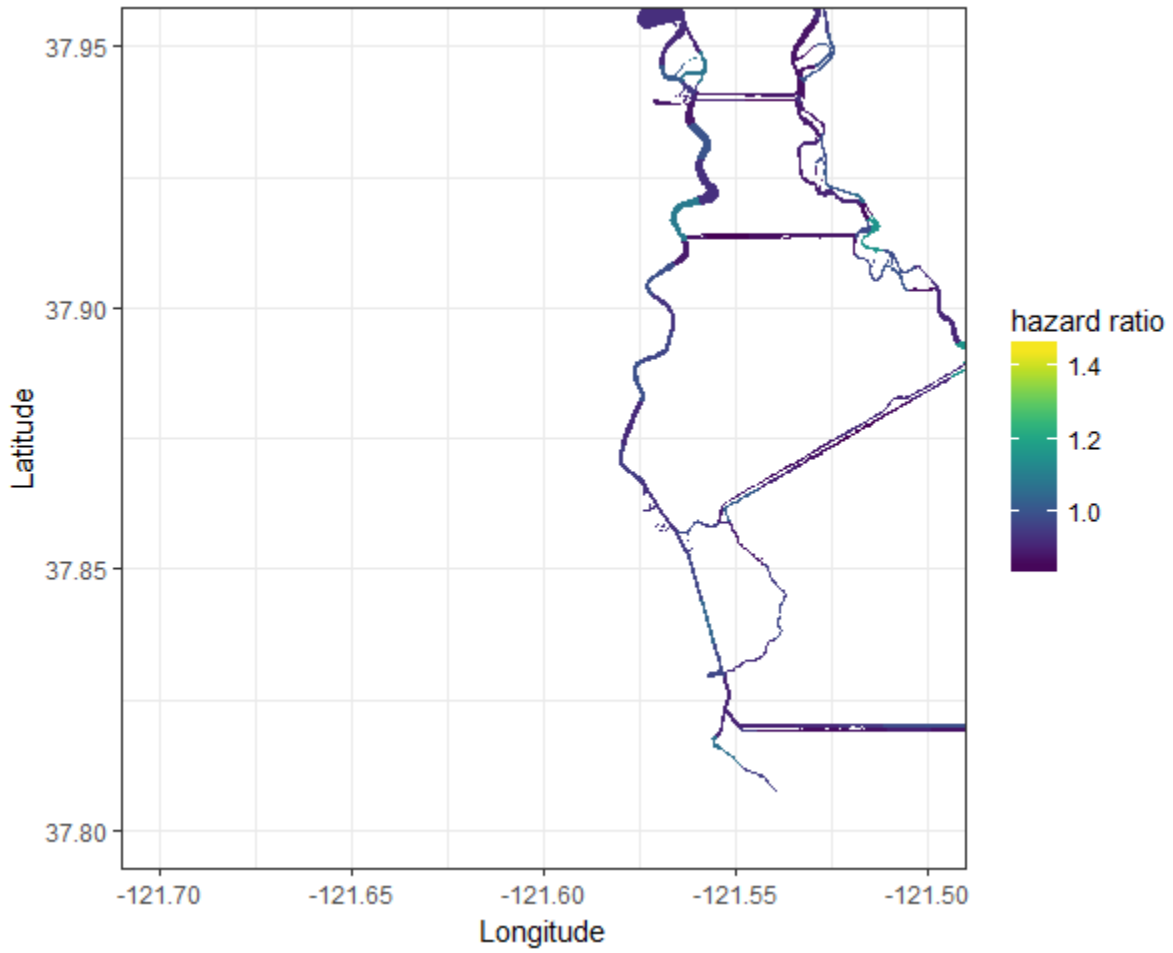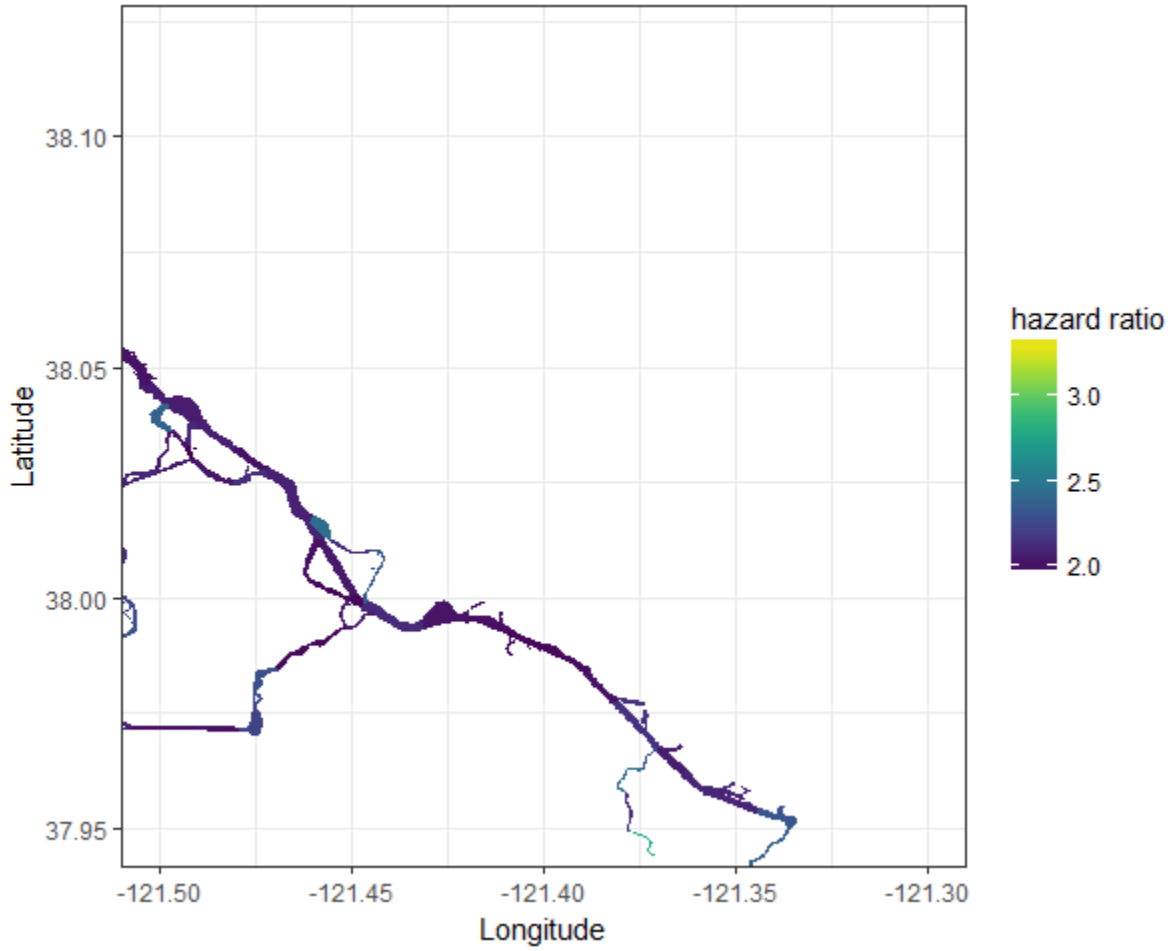
Supplemental Figure 11: 1-km Predation hazard ratio predictions for the 16º (C) temperature scenario, SW quadrant of the South Delta
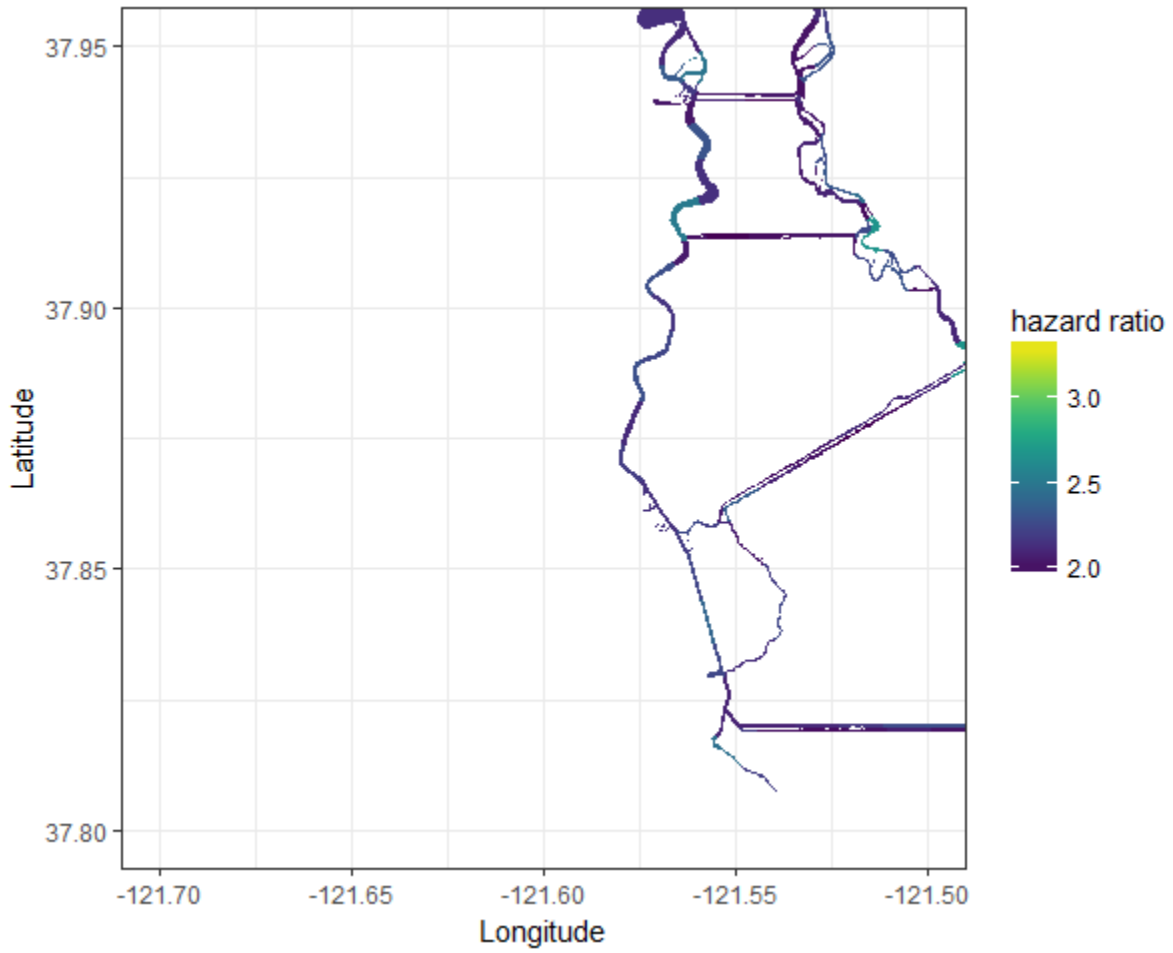
Supplemental Figure 12: 1-km Predation hazard ratio predictions for the 16º (C) temperature scenario, SE quadrant of the South Delta
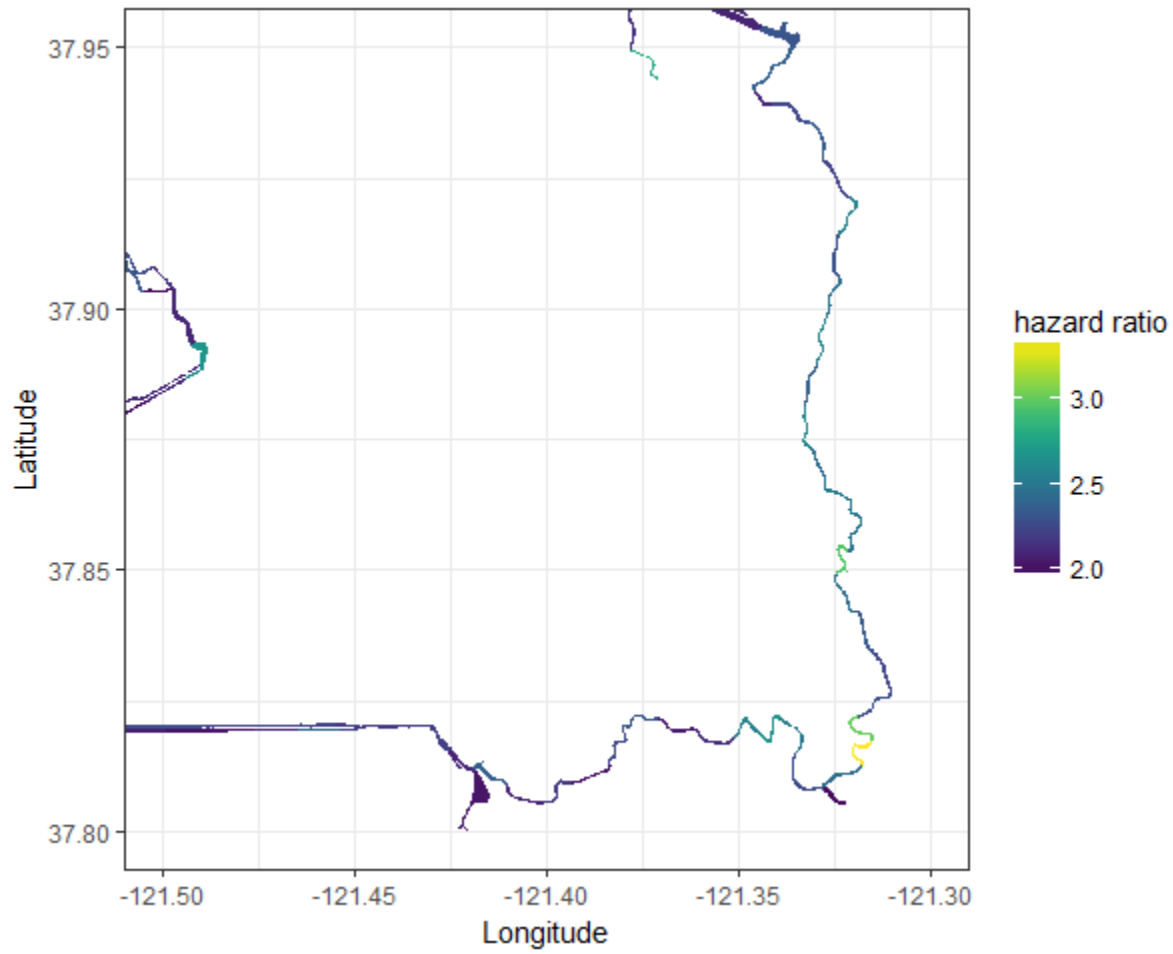
Supplemental Figure 13: 1-km Predation hazard ratio predictions for the 19º (C) temperature scenario, NW quadrant of the South Delta

Supplemental Figure 14: 1-km Predation hazard ratio predictions for the 19º (C) temperature scenario, NE quadrant of the South Delta

Supplemental Figure 15: 1-km Predation hazard ratio predictions for the 19º (C) temperature scenario, SW quadrant of the South Delta

Supplemental Figure 16: 1-km Predation hazard ratio predictions for the 19º (C) temperature scenario, SE quadrant of the South Delta